

5/15/50

# NATIONAL ADVISORY COMMITTEE FOR AERONAUTICS

TECHNICAL NOTE 2098

THE EFFECTS OF STABILITY OF SPIN-RECOVERY TAIL  
PARACHUTES ON THE BEHAVIOR OF AIRPLANES IN  
GLIDING FLIGHT AND IN SPINS.

By Stanley H. Scher and John W. Draper

Langley Aeronautical Laboratory  
Langley Air Force Base, Va.

**DISTRIBUTION STATEMENT A**  
Approved for Public Release  
Distribution Unlimited



Washington

May 1950

Reproduced From  
Best Available Copy

20000801 153

**DTIC QUALITY INSPECTED 4**

AQM00-10-3312

NATIONAL ADVISORY COMMITTEE FOR AERONAUTICS

TECHNICAL NOTE 2098

THE EFFECTS OF STABILITY OF SPIN-RECOVERY TAIL  
PARACHUTES ON THE BEHAVIOR OF AIRPLANES IN  
GLIDING FLIGHT AND IN SPINS

By Stanley H. Scher and John W. Draper

SUMMARY

In several instances during level-flight check tests of the operation of tail spin-recovery parachute equipment, the instability and the erratic behavior of the conventional flat parachutes used caused the airplanes to make uncontrollable gyrations. In order to determine whether a stable parachute could be safely towed behind an airplane in flight and also whether it would be effective as a spin-recovery device, the National Advisory Committee for Aeronautics has conducted an investigation with airplane models in the Langley free-flight and Langley 20-foot free-spinning tunnels. Both hemispherical and flat parachutes with a range of porosities were used in the investigation.

The investigation indicated that when an unstable tail parachute of the size estimated as required for spin recovery was opened from a model in gliding flight, the model performed extremely violent pitching and yawing gyrations which prevented sustained gliding flight; whereas when a stable parachute was opened, the flight characteristics of the model were satisfactory. The gyrations caused by towing unstable parachutes were not reduced appreciably when the towline was lengthened. Satisfactory spin recoveries were effected with either stable or unstable parachutes. In general, the hemispherical parachutes gave spin recoveries equally as good as unstable flat parachutes when the projected diameter of the hemispherical parachute was about two-thirds the laid-out-flat diameter of the unstable flat parachute. The stability of both the hemispherical and flat parachutes was found to be primarily a function of the porosity of the fabric. The parachute drag coefficients decreased as the porosity was increased.

INTRODUCTION

Before some types of airplanes are accepted by the Armed Services, the contractor is required to assure by flight tests that the airplane

is satisfactory with regard to spin recovery. During the spin-demonstration flights, the airplane is usually equipped with a tail parachute for use as an emergency spin-recovery device. The size of parachute and the length of towline needed to provide satisfactory spin recovery for a specific airplane are usually determined by the National Advisory Committee for Aeronautics by means of tests in which small parachutes are opened on a dynamically scaled model of the airplane spinning in the Langley 20-foot free-spinning tunnel. In the past, flat parachutes made of silk or nylon such as is conventionally used in personnel parachutes have been used both in the tunnel tests and in flight and have generally been satisfactory in effecting spin recovery. Recently, however, this type of parachute has caused difficulty when the parachute was opened in normal flight to check the operation of the opening mechanism. After the parachute has been opened, the airplane in several instances has performed wild uncontrollable gyrations and in one instance a fatal crash resulted. This behavior was believed to be caused by the inherent instability of the conventional flat parachute used. In order to verify this fact and to find means for correcting the condition, the NACA has undertaken an investigation with airplane models in the Langley free-flight and Langley 20-foot free-spinning tunnels.

In the investigation, the effect of replacing the unstable flat parachute with a stable parachute in gliding flight and in spins was investigated. The effect of increasing the length of the towline of an unstable flat parachute towed behind a model in a nose-down diving attitude was also studied. The stable parachutes used in the investigation were high-porosity flat and hemispherical parachutes. Before the behavior of the airplane models with the stable parachutes was determined, the stability and drag characteristics of a series of parachutes of different porosities were measured at low speed. Brief tests were also made at high airspeeds on one of the hemispherical parachutes.

#### SYMBOLS

$q$	dynamic pressure, pounds per square foot $\left(\frac{1}{2}\rho V^2\right)$
$V$	airspeed, feet per second
$\rho$	density of air, slugs per cubic foot
$\bar{c}$	mean aerodynamic chord, feet
$x/\bar{c}$	ratio of distance of center of gravity rearward of leading edge of mean aerodynamic chord to length of mean aerodynamic chord

$z/\bar{c}$	ratio of vertical distance between center of gravity and fuselage reference line to length of mean aerodynamic chord (positive when center of gravity is below fuselage reference line)
$k_X, k_Y, k_Z$	radii of gyration about X-, Y-, and Z-axes (body), respectively, feet
$b$	wing span, feet
$S_w$	wing area, square feet
$C_m$	pitching-moment coefficient $\left( \frac{M}{q\bar{c}S_w} \right)$
$C_n$	yawing-moment coefficient $\left( \frac{N}{qbS_w} \right)$
$M$	pitching moment, foot-pounds
$N$	yawing moment, foot-pounds
$C_{n\beta}$	rate of change of yawing-moment coefficient with angle of sideslip per degree $\left( \frac{dC_n}{d\beta} \right)$
$\beta$	angle of sideslip, degrees
$\frac{\partial C_m}{\partial C_L}$	rate of change of pitching-moment coefficient with lift coefficient (static margin)
$C_L$	lift coefficient $\left( \frac{\text{Lift}}{qS_w} \right)$
$C_{L\alpha}$	slope of lift curve per degree $\left( \frac{dC_L}{d\alpha} \right)$
$C_{m\alpha}$	rate of change of pitching-moment coefficient with angle of attack per degree $\left( \frac{dC_m}{d\alpha} \right)$
$\alpha_a$	angle of attack of fuselage reference line of model during gliding flight, degrees
$\alpha_{l_0}$	angle of attack at zero lift, degrees
$\alpha_s$	angle between fuselage reference line and vertical during spin (approximately equal to absolute value of angle of attack at plane of symmetry), degrees

$\Omega$	angular velocity of model about spin axis, revolutions per second
$\gamma$	glide-path angle, degrees
$l_t$	distance from center of gravity of model to parachute-towline attachment point, measured parallel to fuselage reference line, feet
$Z_0$	distance from center of gravity to parachute-towline attachment point, measured perpendicular to fuselage reference line, feet
$H_2$	distance from line of application of parachute drag to center of gravity of model, measured perpendicular to line of application, feet
$H_1$	distance from center of gravity to intersection of towline with vertical body axis, feet (fig. 21)
$A$	distance from attachment point of parachute to intersection of towline with vertical axis, measured perpendicular to X-axis (body), feet (fig. 21)
$C_{Dp}$	drag coefficient of parachute ( $D_p/qS_p$ )
$D_p$	drag of parachute, pounds
$W_p$	weight of parachute including shrouds and towline, pounds
$S_p$	area of parachute, square feet $\left(\frac{\pi d_p^2}{4}\right)$
$d_p$	laid-out-flat diameter of flat parachute; projected diameter of hemispherical parachute
$\epsilon_i$	approximate angle of inclination of parachute from direction of air stream due to its instability, degrees
$\epsilon_w$	approximate angle at which parachute hangs down due to its weight when towed in gliding flight, degrees $\left(\tan^{-1} \frac{W_p}{D_p}\right)$
$\epsilon_p$	approximate total angle of inclination of parachute from direction of air stream, degrees

## APPARATUS

## Wind Tunnels

The tests were made in the Langley free-flight tunnel and in the Langley 20-foot free-spinning tunnel. The Langley free-flight tunnel is equipped for testing free-flying dynamic models and its operation is described in detail in reference 1. An operator adjusts the inclination of the longitudinal axis of the tunnel and the tunnel velocity to correspond to the normal glide-path angle and trim airspeed of the model to control its horizontal and vertical position in the test section. A pilot controls the model in flight by means of two control sticks that supply current to small, electromagnetic mechanisms within the model that actuate the control surfaces. The motions of the model are observed by the pilot in order to determine its stability and control characteristics. These observations are supplemented by motion-picture records. The Langley 20-foot free-spinning tunnel has a vertically rising air stream and its operation is similar to that described in reference 2 for the Langley 15-foot free-spinning tunnel, except that the dynamic models are launched by hand with spinning rotation rather than launched from a spindle. The airspeed is adjusted to equal the rate of descent of a spinning model. Fully developed spins are studied and an attempt is then made to effect recovery from the spin by control reversal, opening a spin-recovery parachute, or by some other recovery device.

## Airplane Models

One free-flight-tunnel model, which is referred to herein as model 1, and five free-spinning-tunnel models, which are referred to herein as models 2 to 6, were used in the tests. Three-view drawings of the models are shown in figures 1 to 6. The general construction of the models, which were made principally of balsa, is described in references 1 and 2. The models were ballasted with lead weights and dynamically represented airplanes such as fighters and torpedo-bomber airplanes which might use a spin-recovery parachute. The model loading conditions are listed in table I. Remote-control mechanisms were installed in each model to open the parachutes.

## Parachutes

The flat spin-recovery parachutes used in the investigation were made of circular pieces of nylon, silk, or loosely woven mesh. The nylon and silk parachutes had central vents and were similar in construction to those described in reference 3. The flat parachutes used are listed in table II and photographs of a typical unstable flat parachute inflated are presented as figure 7.

The hemispherical parachutes had preformed hemispherical canopy shapes with the diameters ranging from 4.14 inches to 36.56 inches (projected diameters); they were made of different types of cloth, the specified porosity numbers of which ranged from 150 to over 900. The porosity numbers are given as the cubic feet of air that will pass through 1 square foot of the cloth per minute under a pressure of 1/2 inch of water. The porosity as given for each parachute does not take into account a probable reduction in air flow through the parachute due to seam construction between the panels or due to the double-thickness crown panel which was at the top of each parachute canopy. The hemispherical parachutes used are listed in table III and a photograph of a stable hemispherical parachute inflated is presented as figure 8.

#### METHODS AND TESTS

Two testing methods were used to study the stability of the various parachutes. One method consisted of tying the end of the towline of each parachute listed in table IV to a bar, holding the bar in the air stream of the Langley 20-foot free-spinning tunnel, and noting the behavior of the parachute over the range of airspeeds noted in table IV. The other method consisted of tying weights to the towline of each of the parachutes listed in table V, releasing it to float freely in the air stream of the Langley 20-foot free-spinning tunnel, and noting the behavior of the parachute. Parachutes which aligned themselves with the wind stream were considered to be completely stable, although parachutes which inclined only a few degrees from the air stream and did not oscillate were also classified as stable. In order to obtain data for calculating the drag coefficients of the parachutes, the airspeed necessary to hold the parachutes and weights at test level when they were floating freely in the Langley 20-foot free-spinning tunnel was recorded. The drag of the parachute was then taken to be equal to the sum of the weight of the parachute and the suspended weight.

In the gliding-flight tests in the Langley free-flight tunnel, unstable and stable parachutes of various sizes as listed in table VI were opened on a 30-inch towline attached to the tail cone of model 1 while the model was in flight, and the glide-path angle and air-stream velocity were adjusted to the resulting new trim conditions. Observations of the stability of each parachute and the resulting effects on the stability and control of the model were made. A photograph showing the model towing a stable hemispherical parachute is given as figure 9.

For the spin-recovery tests, made with models 2 to 5, the parachute pack was installed near the rear of the fuselage below the horizontal tail and the towline was attached to the rear of the fuselage. The parachutes and towlines used on each model are indicated in table VII.

Various airplane tail-parachute installations are discussed in reference 4. A typical free-spinning-tunnel model is shown spinning in the tunnel in figure 10. The number of turns required for recovery from the spins was measured from the time the parachute pack was freed to permit its opening for recovery until the spin rotation ceased.

Tests were made to determine the effect of parachute-towline length on the behavior of a diving model towing an unstable flat tail parachute. For these tests, model 6 was suspended in the vertical air stream of the Langley 20-foot free-spinning tunnel from the 10.00-inch-diameter unstable flat parachute with successive towlines of 10 inches, 30 inches, and 60 inches attached to the rear of the fuselage. The behavior of the parachute and of the model in the air stream were noted.

The 11.84-inch-diameter 400-porosity hemispherical parachute was tested in the Langley 300 MPH 7- by 10-foot tunnel at airspeeds up to 246 miles per hour to determine the opening characteristics of the parachute at high speed.

Motion pictures were taken during the various tests and the film records were used in evaluating the results.

## RESULTS AND DISCUSSION

### Preliminary Study of Parachute Characteristics

Parachute stability.- The results of the tests made to determine the stability of the parachutes are presented in tables IV and V. The average angle of inclination of the parachute to the air stream  $\epsilon_1$  varied with porosity as shown in figure 11. A porosity of at least 400 was necessary to make the hemispherical parachutes remain stably alined within a few degrees of the direction of the air stream. As the porosity was decreased below 400, the parachutes became unstable and inclined progressively more and more from the direction of the air stream and began to make erratic side-to-side motions. The 400-porosity hemispherical parachutes were selected as sufficiently stable for use in the tests of the gliding-flight and spin-recovery models. It was found that a flat parachute of very high porosity alined itself stably with the air stream, just as did the high-porosity hemispherical parachutes. The stability of the parachutes was not appreciably affected by changes in airspeed over the test range indicated in tables IV and V. A photograph of five approximately 9.80-inch-diameter hemispherical parachutes of different porosities (ranging from 150 to 400) with their towlines attached to a horizontal bar in the air stream is presented as figure 12. Motion-picture strips of two 5.86-inch-diameter hemispherical parachutes, one with a porosity

of 150 and one with a porosity of 400, floating freely in the air stream are presented in figures 13 and 14, respectively. The results of the tests made over the porosity range of 30 to 294 indicate that the hemispherical shape contributed somewhat to the parachute stability because the unstable hemispherical parachutes within that porosity range occasionally ceased their erratic motions for a brief instant and merely traveled across the tunnel, whereas the 120-porosity flat parachutes were continuously erratic.

The present test results are in agreement with the results presented in an unavailable British paper, wherein it is noted that porosity has a large effect on the stability of a parachute. That the shape of a parachute may also affect its stability is indicated by the present test results, by those reported in the aforementioned British paper, by the results reported in reference 5, and by a few tests (results unpublished) with truncated pyramidal parachutes. The present results obtained with the 9.80-inch-diameter 400-porosity hemispherical parachute with shortened shroud lines (table IV) are in agreement with the British paper, which indicates that parachute stability is independent of both the length and number of shroud lines.

Parachute drag coefficients.- The drag coefficients measured for the hemispherical and flat parachutes of various porosities are given in table V and are plotted for the hemispherical parachutes in figure 15. The value of drag coefficient at zero porosity plotted in figure 15 for comparison was obtained from reference 6 for a metal hemispherical shell. It will be noted from figure 15 that the drag coefficients decreased as the porosity was increased. The drag coefficient of the hemispherical parachute of sufficient porosity to provide stability (porosity of 400) was 1.1 as compared with 1.4 for the metal hemispherical shell. These coefficients are based on the projected area of the canopy. The drag coefficients of the flat parachutes given in table V are based on the surface area. For a direct comparison with the flat parachutes in terms of surface area, the drag coefficients of the hemispherical parachutes should be divided by 2. On this basis the 400-porosity stable hemispherical parachute had a drag coefficient of 0.55 as compared with 0.71 for the conventional flat parachute, and for equal drag at a given airspeed, the hemispherical parachute would require approximately 130 percent of the surface area of the conventional parachute. The corresponding projected area of the hemispherical parachute would then be 65 percent of the surface area of the conventional parachute and the corresponding projected diameter specified for the hemispherical parachute would be approximately 80 percent that of the laid-out-flat diameter of the conventional parachute.

Parachute behavior as affected by airspeed.- Over the airspeed range tested (velocity range, 26 to 92 fps) with the parachute towlines tied to a bar in the air stream of the Langley 20-foot free-spinning tunnel (table IV),

the hemispherical parachutes having porosities of 150 to 400 retained their shape and the 120-porosity flat parachute retained its fully inflated shape. The parachutes having porosities greater than 400, however, including both the hemispherical and flat parachutes, started to close at the rim as the airspeed was increased above 26 feet per second. At 40 feet per second the hemispherical parachute with a porosity of 612 was nearly closed. With a strip of imporous tape  $3/4$  inch wide attached around the rim of the 612-porosity hemispherical parachute just above the hem (hem was  $1/4$  in. wide), the parachute remained fully open in a hemispherical shape over the entire airspeed test range. A strip of tape 1 inch wide applied in a similar manner to the 10.60-inch-diameter flat parachute made of loosely woven mesh caused it also to remain fully open over the entire airspeed range.

In the tests of the 11.84-inch-diameter 400-porosity stable hemispherical parachute in the Langley 300 MPH 7- by 10-foot tunnel, it was found that the hemispherical parachute retained its shape as the tunnel airspeed was increased from low speed to an indicated sea-level velocity of 361 feet per second (246 mph). However, when the same parachute was opened at an indicated sea-level velocity of 304 feet per second (208 mph), it contracted at the hem and assumed a pear shape which it retained as the airspeed was decreased to zero. When this parachute was opened in the Langley 20-foot free-spinning-tunnel air stream at an airspeed of 92 feet per second, it assumed a hemispherical shape. Measured drag coefficients of the parachute at various indicated sea-level velocities during the test runs in the Langley 300 MPH 7- by 10-foot tunnel are plotted in figure 16. As shown in the figure, the drag coefficients depended on the shape of the parachute and were smaller when the parachute was pear-shaped than when it was open to its full hemispherical shape. For both the pear shape and the hemispherical shape the parachute drag coefficients increased with a decrease in airspeed.

Experience with full-scale hemispherical parachutes of the particular type used in the model tests has indicated that the pear shape is normally obtained upon opening at high speeds and that the final hemispherical shape usually develops soon after the airspeed is reduced. With regard to airplane spin recovery, the airspeed is not appreciably reduced after the parachute opens and therefore a parachute which is selected as sufficient to provide spin recovery should open fully almost immediately so that all its potential drag will act to effect rapid spin recovery. The opening characteristics of full-scale stable spin-recovery parachutes can best be determined by testing them at the airspeeds attained by airplanes in spins. The results of a wind-tunnel investigation of the effects of several parachute design variables on the opening characteristics of a series of hemispherical parachutes are presented in reference 7.

### Behavior in Gliding Flight

The results of the tests in which unstable and stable tail parachutes were opened on model 1 during gliding flight in the Langley free-flight tunnel are presented in table VI. The comparative behavior of stable and unstable parachutes being towed behind the model in gliding flight is shown in the motion-picture strips in figure 17. Opening unstable parachutes of either the conventional flat type or the low-porosity hemispherical type had an adverse effect on the stability of the model because of the erratic oscillatory motions of the parachute. When the unstable parachute was small, its erratic motions caused little difficulty in flying the model because the forces exerted on the model were small. With the larger unstable parachutes, however, the forces were large enough to impart severe and erratic pitching and yawing motions which made sustained flight difficult or impossible. A 7.00-inch-diameter flat parachute and a 7.26-inch-diameter hemispherical parachute of nearly equivalent porosity were the largest of the lower-porosity unstable parachutes with which flight could be maintained. When a 15-inch-diameter flat parachute - the size estimated as necessary for satisfactory spin recovery - was opened, the model performed extremely violent pitching and yawing gyrations which prevented sustained gliding flight. When stable parachutes were opened, there was no adverse effect on the flying characteristics of the model; rather, the primary effect of the stable parachute was to increase the stability of the model. A method of calculating the increase in longitudinal and directional stability of the model contributed by the parachute is presented in the appendix. The changes in glide-path angles and trim lift coefficients for the different parachutes with the towline attachment at the rear of the fuselage as shown in figure 1 are also presented in table VI. The main effect of opening a parachute was to steepen the glide-path angle without much change in the trim lift coefficient. The maximum change in glide-path angle observed was  $14^\circ$  which was obtained with the 9.86-inch-diameter 200-porosity hemispherical parachute. A method of estimating the effect of the parachute on the trim lift coefficient, which is a function of the aerodynamic characteristics of the airplane and parachute as well as the geometry of the installation, is given in the appendix.

### Spin-Recovery Effectiveness

The results of the spin-recovery-parachute tests are presented in table VII. The calculated drag of each open parachute during the spin recovery is also included in the table. The drag coefficients used in calculating the drag were taken from table V. Motion-picture strips showing model 5 recovering from spins after a parachute was opened are shown in figures 18 and 19. The respective parachutes shown are

the 6.00-inch-diameter unstable flat type and the 4.20-inch-diameter 400-porosity stable hemispherical type, and both recoveries shown were effected in about 1 turn of the model. As the model dived following the recoveries from the spin, the flat parachute moved from side to side behind the model, whereas the 400-porosity hemispherical parachute trailed stably behind the model. The results obtained with models 2 and 5 indicate that there was no appreciable difference in the number of turns for recovery required after opening a stable hemispherical parachute (porosity 400) or an unstable hemispherical parachute (porosity 150) of the same diameter and of approximately the same drag. (See table VII.) When an unstable flat parachute of 9.00-inch laid-out-flat diameter and a hemispherical parachute of 5.86-inch projected diameter were opened for spin recovery on models 2, 3, and 4, the results were as follows: For model 2, recoveries obtained with the flat parachute appeared to be slightly better than those obtained with the hemispherical parachute; for model 3, the turns required for recovery with the flat and hemispherical parachutes were not appreciably different; for model 4, the recoveries obtained with the hemispherical parachute were better than those obtained with the flat parachute. Also, for model 5, a 4.20-inch-diameter hemispherical parachute effected slightly better recoveries than did a 6.00-inch-diameter flat parachute. It appears, therefore, that in general the hemispherical parachute gave spin recoveries equally as good as flat parachutes when the projected diameter of the hemispherical parachute was about two-thirds the laid-out-flat diameter of the flat parachute. The drag of the hemispherical parachutes required for recovery was approximately 70 percent of the drag of the flat parachute.

For model 4, the recoveries obtained with the 10.60-inch-diameter high-porosity stable flat parachute were better than those obtained with the 9.00-inch-diameter unstable flat parachute, even though the drag of the stable parachute was less than that of the unstable parachute.

#### Effect of Increasing Towline Length

When model 6 was tested in the Langley 20-foot free-spinning tunnel at an airspeed of approximately 57.5 feet per second in a nose-down diving attitude with the 10.00-inch-diameter unstable flat parachute attached to the tail with a 10-inch towline, the erratic behavior of the unstable parachute caused the model to make violent pitching and yawing gyrations of as much as  $30^\circ$  from a vertical nose-down attitude. The actions of the model and the parachute during tests with the 10-inch towline are shown in the motion-picture strip in figure 20. When the towline length was 60 inches, the gyrations of the model were slightly less violent than when the towline length was 10 inches. If it is assumed that the model represented an airplane with a wing span of 50 feet,

the full-scale parachute diameter was 26.2 feet, and the full-scale towline lengths were 26.2 feet and 157 feet, respectively. The results of the tests indicate that increasing the towline length will not eliminate the difficulties associated with towing unstable parachutes.

#### CONCLUDING REMARKS

Based on the results of an investigation with airplane models in the Langley free-flight and Langley 20-foot free-spinning tunnels to determine whether a stable parachute could be safely towed behind an airplane in flight and also whether it would be effective as a spin-recovery device, the following concluding remarks can be made:

1. When unstable tail parachutes of the size estimated as required for spin recovery were opened from a model in gliding flight, sustained flight was impossible because of the extremely violent pitching and yawing gyrations performed by the model.

2. When stable tail parachutes of the size required for spin recovery were opened in gliding flight, the stability of the model was increased and sustained flights could be made with ease.

3. Satisfactory spin recoveries were effective with either stable or unstable parachutes.

4. In general, the hemispherical parachutes gave spin recoveries equally as good as unstable flat parachutes when the projected diameter of the hemispherical parachute was about two-thirds the laid-out-flat diameter of the flat parachute.

5. The gyrations which the model made when towing an unstable tail parachute were not appreciably lessened by increasing the length of the towline.

6. The stability of the parachutes was found to be primarily a function of porosity of the fabric.

7. The parachute drag coefficients decreased as the porosity was increased.

Langley Aeronautical Laboratory  
National Advisory Committee for Aeronautics  
Langley Air Force Base, Va., June 23, 1948

## APPENDIX

## FORMULAS FOR ESTIMATING THE EFFECT OF TAIL

## PARACHUTES ON AIRPLANE STABILITY

A tail parachute theoretically increases the static longitudinal and directional stability of an airplane. In practice, however, this increase is not realized if the parachute itself is unstable. For the case of the stable tail parachute, the increases in the static stability of the airplane may be estimated from the formulas derived in the following paragraphs. The symbols used are explained in figure 21.

Static longitudinal stability. - The increment in pitching moment produced by a tail parachute is

$$\Delta M = D_p H_2 \quad (1)$$

From figure 21,

$$H_2 = H_1 \cos (\alpha_a - \epsilon_p) \quad (2)$$

where

$$H_1 = Z_o - A \quad (3)$$

and

$$A = l_t \tan (\alpha_a - \epsilon_p) \quad (4)$$

For small values of  $\alpha_a - \epsilon_p$ ,

$$H_2 = H_1 = Z_o - l_t (\alpha_a - \epsilon_p) \quad (5)$$

The total parachute inclination angle  $\epsilon_p$  can be broken down into its component parts as follows:

$$\epsilon_p = (\alpha_a - \alpha_{l_0}) \frac{d\epsilon_p}{d\alpha} + \epsilon_W + \epsilon_1 \quad (6)$$

where  $\epsilon_W$  is the approximate angle at which the parachute hangs down because of its weight and is calculated by the simple relation

$$\epsilon_W = \tan^{-1} \frac{W_p}{D_p} \quad (7)$$

The term  $\epsilon_1$  is the angle at which the parachute hangs down because of its instability. It has already been shown (fig. 11) that in a vertically rising air stream, parachutes are inclined at some angle to the air stream and the angle of inclination increases as the porosity is decreased. In a horizontal air stream this inclination is also present and is usually downward because of the weight of the parachute. Tests of parachutes in the Langley free-flight tunnel indicated that  $\epsilon_1$  varied with porosity in approximately the same manner that the inclination angle varied in the vertical air stream. Values of  $\epsilon_1$  for parachutes of different porosity can therefore be obtained directly from figure 11.

Substituting in equation (5) the expression for  $\epsilon_p$  given in equation (6) gives

$$H_2 = Z_0 - l_t \left[ \alpha_a \left( 1 - \frac{d\epsilon_p}{d\alpha} \right) + \alpha_{l_0} \frac{d\epsilon_p}{d\alpha} - \epsilon_W - \epsilon_1 \right] \quad (8)$$

Converting to coefficient form and substituting the value of  $H_2$  shown in equation (8) gives

$$\Delta C_m = C_{Dp} \frac{S_p}{S_w} \frac{1}{c} \left\{ Z_0 - l_t \left[ \alpha_a \left( 1 - \frac{d\epsilon_p}{d\alpha} \right) + \alpha_{l_0} \frac{d\epsilon_p}{d\alpha} - \epsilon_W - \epsilon_1 \right] \right\} \quad (9)$$

Differentiating equation (9) with respect to angle of attack ( $\alpha_a$ ) gives  $\Delta C_{m_\alpha}$  (per radian) as

$$\Delta C_{m_\alpha} = - C_{Dp} \frac{S_p}{S_w} \frac{l_t}{c} \left( 1 - \frac{d\epsilon_p}{d\alpha} \right) \quad (10)$$

Dividing equation (10) by  $C_{L\alpha}$  (per radian) gives the incremental static-margin factor  $\Delta \frac{\partial C_m}{\partial C_L}$ ,

$$\Delta \frac{\partial C_m}{\partial C_L} = - \frac{C_{Dp}}{C_{L\alpha}} \frac{S_p}{S_w} \frac{l_t}{\bar{c}} \left( 1 - \frac{d\epsilon_p}{d\alpha} \right) \quad (11)$$

The rate of change of downwash with angle of attack  $\frac{d\epsilon_p}{d\alpha}$  was determined experimentally to be approximately 0.2 for model 1 for the towline lengths used. This value was used in calculating the longitudinal stability increment caused by the parachute.

Static directional stability.- Similar treatment of the directional stability results in the following expression:

$$\Delta C_{n\beta} = C_{Dp} \frac{S_p}{S_w} \frac{l_t}{b} \quad (\text{per radian}) \quad (12)$$

(Sidewash was not taken into account in this expression.)

Calculated changes in stability.- In order to illustrate the effect of a tail parachute on the stability of model 1, calculations were made by using equations (11) and (12). The calculations were made for a 7.23-inch-diameter 400-porosity hemispherical parachute. The results showed that the static margin  $\partial C_m / \partial C_L$  was increased by -0.11 and the static directional stability  $C_{n\beta}$  was increased by 0.0014 per degree.

Calculated changes in trim.- The change in trim lift coefficient  $\Delta C_L$  caused by the opening of a tail parachute can be calculated by dividing the value of  $\Delta C_m$  obtained from equation (9) by the total static margin  $\partial C_m / \partial C_L$  which is obtained by adding the incremental static margin calculated by equation (11) to the static margin of the airplane without the parachute.

For the parachute having large values of  $\epsilon_1$  and erratic motions (porosity under 250) the change in trim cannot be calculated accurately by this method.

Calculations were made by this method to determine the change in trim for model 1 when a 7.23-inch-diameter 400-porosity hemispherical parachute was attached at the tail at a special attachment point 4.7 inches below the center of gravity. The results indicated a change in trim lift coefficient of -0.16 which agreed fairly well with the change of -0.19 observed in flight tests of this condition.

## REFERENCES

1. Shortal, Joseph A., and Osterhout, Clayton J.: Preliminary Stability and Control Tests in the NACA Free-Flight Wind Tunnel and Correlation with Full-Scale Flight Tests. NACA TN 810, 1941.
2. Zimmerman, C. H.: Preliminary Tests in the N.A.C.A. Free-Spinning Wind Tunnel. NACA Rep. 557, 1936.
3. Kamm, Robert W., and Malvestuto, Frank S., Jr.: Comparison of Tail and Wing-Tip Spin-Recovery Parachutes as Determined by Tests in the Langley 20-Foot Free-Spinning Tunnel. NACA ARR L5G19a, 1946.
4. Seidman, Oscar, and Kamm, Robert W.: Antispin-Tail-Parachute Installations. NACA RB, Feb. 1943.
5. Wood, John H.: Determination of Towline Tension and Stability of Spin-Recovery Parachutes. NACA ARR L6A15, 1946.
6. Brevoort, M. J., and Joyner, U. T.: Aerodynamic Characteristics of Anemometer Cups. NACA TN 489, 1934.
7. Scher, Stanley H., and Gale, Lawrence J.: Wind-Tunnel Investigation of the Opening Characteristics, Drag, and Stability of Several Hemispherical Parachutes. NACA TN 1869, 1949.

TABLE I  
LOADING CONDITIONS OF THE AIRPLANE MODELS USED  
IN TAIL-PARACHUTE STABILITY INVESTIGATION

Model	Weight (lb)	Center-of-gravity location		$\frac{k_X}{b}$	$\frac{k_Y}{b}$	$\frac{k_Z}{b}$
		$x/\bar{c}$	$z/\bar{c}$			
1	7.93	0.282	0.006	(a)	(a)	(a)
2	3.69	.268	.001	0.110	0.157	0.192
3	3.35	.251	.010	.111	.141	.178
4	2.35	.284	.017	.119	.122	.167
5	1.50	.230	.017	.100	.203	.220
6	2.09	.231	-.031	.101	.158	.181

<sup>a</sup>Values not measured.



TABLE II

## FLAT PARACHUTES USED IN TAIL-PARACHUTE

## STABILITY INVESTIGATION

Parachute diameter, $d_p$ <sup>a</sup> (in.)	Canopy material	Porosity of canopy material <sup>b</sup>	Vent diameter, $d_p/12$ (in.)	Number of shroud lines	Length of shroud lines (in.)
4.25	Silk	<sup>c</sup> Approx. 120	0.35	8	5.74
5.70	----do----	<sup>c</sup> Approx. 120	.48	8	7.70
6.00	----do----	<sup>c</sup> Approx. 120	.50	8	8.10
7.00	----do----	<sup>c</sup> Approx. 120	.58	8	9.45
8.00	----do----	<sup>c</sup> Approx. 120	.67	8	10.80
9.00	----do----	<sup>c</sup> Approx. 120	.75	10	12.15
10.00	Nylon	<sup>c</sup> Approx. 120	.83	8	13.50
10.60	Loosely woven mesh	<sup>d</sup> Very high	None	8	14.30
14.00	Silk	<sup>c</sup> Approx. 120	1.17	8	18.90

<sup>a</sup>Laid-out-flat diameter.<sup>b</sup>Cubic feet of air flow per minute through 1 square foot of material under pressure of 1/2 inch of water.<sup>c</sup>Parachutes were made from parachute silk and nylon, the porosities of which were based on specifications of the Armed Services.<sup>d</sup>Porosity of this parachute was not measured but probably exceeded 900.

TABLE III

## HEMISPHERICAL PARACHUTES USED IN TAIL-PARACHUTE

## STABILITY INVESTIGATION

[Parachutes were made of silk or nylon unless otherwise noted  
and had no central vent]

Parachute diameter <sup>a</sup> (in.)	Porosity of canopy material <sup>b</sup> (cu ft/sq ft/min)	Number of shroud lines	Length of shroud lines (in.)
4.14	150	12	12.75
4.20	250	12	12.75
4.20	400	12	12.75
5.86	150	12	18.00
5.86	250	12	18.00
5.86	400	12	18.00
7.26	150	16	22.50
7.20	200	16	22.50
7.20	294	16	22.50
7.23	400	16	22.50
8.28	150	16	25.50
8.21	200	16	25.50
8.35	250	16	25.50
8.21	294	16	25.50
8.35	400	16	25.50
10.10	<sup>c</sup> Approx. 0	16	30.00
9.86	150	16	30.00
9.86	200	16	30.00
9.86	250	16	30.00
9.86	294	16	30.00
9.80	400	16	30.00
9.86	432	16	20.00
9.80	460	16	20.00
9.86	543	16	20.00
9.80	612	16	20.00
10.00	<sup>d</sup> 700	16	20.00
9.80	>900	16	20.00
11.78	150	16	36.00
11.57	200	16	36.00
11.52	250	16	36.00
11.78	294	16	36.00
11.84	400	16	36.00
24.20	157	16	29.00
36.56	30	16	41.80

<sup>a</sup>Preformed diameter.

<sup>b</sup>Measured by manufacturer.

<sup>c</sup>Parachute made at the Langley Laboratory of layers of gauze impregnated with airplane dope (cellulose nitrate) thinned with acetone.

<sup>d</sup>Parachute made of nylon screen; porosity too high to be measured with manufacturer's measuring device.



TABLE IV  
 STABILITY OF PARACHUTES WITH END OF  
 TOWLINE TIED TO BAR IN AIR STREAM  
 [V range, 26 to 92 fps]

Parachute			Stability of parachute	
Type	Diameter <sup>a</sup> (in.)	Porosity of material (cu ft/sq ft/min)	Behavior in air stream	$\epsilon_1$ (deg)
Hemispherical	4.20	400	Stable; alined within a few degrees of direction of air stream	3 to 5
Do-----	5.86	400	-----do-----	3 to 5
Do-----	7.23	400	-----do-----	3 to 5
Do-----	8.35	400	-----do-----	3 to 5
Do-----	9.80	400	-----do-----	3 to 5
Do-----	<sup>b</sup> 9.80	400	Stable; alined within a few degrees of direction of air stream; slight vibrations in canopy which were not present with the longer shroud lines	3 to 5
Do-----	11.84	400	Stable; alined within a few degrees of direction of air stream	3 to 5
Do-----	10.10	0	Circled erratically while leaning to side	48
Do-----	9.86	150	Moved erratically back and forth and from side to side	15 to 20
Do-----	9.86	200	-----do-----	10 to 12
Do-----	9.86	250	-----do-----	4 to 8
Do-----	9.86	294	-----do-----	6 to 10
Do-----	9.86	432	Stable; alined within a few degrees of direction of air stream	2 to 4
Do-----	9.80	460	Stable; alined within a few degrees of direction of air stream	1 to 3
Do-----	9.86	543	Stable; alined with air stream	0
Do-----	9.80	612	-----do-----	0
Do-----	10.00	700	-----do-----	0
Do-----	9.80	>900	-----do-----	0
Do-----	8.28	150	Moved erratically back and forth and from side to side	15 to 20
Do-----	8.21	200	-----do-----	10 to 12
Do-----	8.35	250	-----do-----	4 to 8
Do-----	8.21	294	-----do-----	6 to 10
Do-----	11.78	150	-----do-----	15 to 20
Do-----	11.57	200	-----do-----	10 to 12
Do-----	11.52	250	-----do-----	4 to 8
Do-----	11.78	294	-----do-----	6 to 10
Flat	8.00	Approx. 120	Moved back and forth and from side to side or circled erratically while leaning to side	28 to 32
Do-----	10.00	Approx. 120	-----do-----	28 to 32
Do-----	14.00	Approx. 120	-----do-----	28 to 32
Do-----	10.60	Very high	Stable; alined with air stream	0

<sup>a</sup>Preformed diameter for hemispherical parachutes; laid-out-flat diameter for flat parachutes.

<sup>b</sup>Shroud lines shortened in length from 30 inches (table III) to 10 inches.



TABLE V  
STABILITY AND DRAG CHARACTERISTICS OF PARACHUTES  
FLOATING FREELY IN AIR STREAM

Parachute			Stability of parachute		Drag characteristics of parachute				
Type	Diameter <sup>a</sup> (in.)	Porosity (cu ft/sq ft/min)	Behavior in air stream	$\epsilon_i$ (deg)	$W_p$ (lb)	Suspended weight (lb)	$D_p$ (lb)	$V$ (fps)	$C_{Dp}$
Hemi- spherical	9.86	150	Made erratic motions, leaning from side to side; traveled across or around tunnel	20	0.039	1.103	1.142	38.7	1.818
Do-----	9.86	200	-----do-----	15	.039	1.103	1.142	37.2	1.677
Do-----	9.86	250	Less erratic than 150-porosity	5 to 10	.039	1.103	1.142	38.7	1.815
Do-----	9.86	204	9.86-inch parachute	5 to 10	.049	1.103	1.152	38.0	1.749
Do-----	9.80	400	-----do-----	3 to 5	.046	1.103	1.149	40.2	1.19
Do-----	9.80	400	Stable; aligned within a few degrees of direction of air stream	3 to 5	.046	.441	.487	25.3	.783
Do-----	9.86	432	-----do-----	2 to 4	.038	.441	.479	27.3	.912
Do-----	9.80	460	-----do-----	1 to 3	.030	.441	.471	27.3	.985
Do-----	9.86	543	-----do-----	0	.031	.441	.472	27.3	.912
Do-----	9.80	612	Stable; aligned with air stream	0	.051	.441	.492	30.1	1.109
Do-----	10.00	700	-----do-----	0	.040	.441	.481	27.3	.968
Do-----	9.80	>900	-----do-----	0	.061	.441	.502	30.1	.864
Do-----	5.86	150	Made erratic motions, leaning from side to side; traveled across or around tunnel	20	.022	.276	.298	33.6	1.165
Do-----	5.86	250	Less erratic than 150-porosity	10 to 15	.024	.276	.300	33.6	1.172
Do-----	5.86	400	5.86-inch parachute	3 to 5	.027	.276	.303	33.6	1.167
Do-----	5.86	400	Stable; aligned within a few degrees of direction of air stream	3 to 5	.028	.441	.469	42.2	1.161
Do-----	4.14	150	-----do-----	20	.015	.324	.339	49.8	1.215
Do-----	4.20	250	Made erratic motions, leaning from side to side; traveled across or around tunnel	5 to 10	.015	.324	.339	49.1	1.211
Do-----	4.20	400	Less erratic than 150-porosity	3 to 5	.015	.324	.339	49.8	1.174
Do-----	24.20	157	4.14-inch parachute	-----	.100	4.350	4.450	31.4	1.159
Do-----	36.56	30	Stable; aligned within a few degrees of direction of air stream	-----	.269	4.160	4.429	20.4	1.307
Flat	9.00	Approx. 120	Made erratic motions, leaning from side to side; traveled across or around tunnel	30	.004	.441	.445	34.3	1.425
Do-----	8.00	Approx. 120	-----do-----	30	.004	.441	.445	38.7	b .704
Do-----	6.00	Approx. 120	-----do-----	30	.003	.324	.327	43.6	b .724
Do-----	c 10.60	Probably >900	-----do-----	0	.001	.441	.442	42.2	b .341

<sup>a</sup>Preformed diameter for hemispherical parachutes; laid-out-flat diameter for flat parachutes.

<sup>b</sup>Values given are based on laid-out-flat diameters of 9.00, 8.00, 6.00, and 10.60 inches, respectively; if based on approximate inflated diameters (6.25, 5.50, 4.20, and 7.25 inches, respectively), the drag coefficients would be 1.470, 1.489, 1.478, and 0.726.

<sup>c</sup>This parachute had a strip of imporous tape 1 inch wide attached around its edge just above the rim.



TABLE VI  
STABILITY AND CONTROL CHARACTERISTICS OF AN AIRPLANE MODEL IN GLIDING FLIGHT IN THE  
LANGLEY FREE-FLIGHT TUNNEL WHILE TOWING DIFFERENT TYPES OF  
TAIL SPIN-RECOVERY PARACHUTES

[Without parachute:  $C_L = 0.8$ ,  $\gamma = 8.9^\circ$ ,  $V = 54$  fps; 30-inch towline used for all tests]

$d_p$ (in.) (approx.)	Flat type		Hemispherical type															
	Porosity		Porosity															
	Approx. 120		150				200				294				400			
	P (a)	M (b)	$\Delta C_L$ (c)	$\Delta \gamma$ (d)	P	M	$\Delta C_L$	$\Delta \gamma$	P	M	$\Delta C_L$	$\Delta \gamma$	P	M	$\Delta C_L$	$\Delta \gamma$	P	M
4.2	D	B	-----	-----	D+	B+	-0.01	3.0	-	-	-----	-----	-	-	-----	3.3	A	A
5.7	D	C	-0.19	5.25	--	--	-----	-----	-	-	-----	-----	-	-	-----	-----	-	-
5.9	--	--	-----	-----	D+	C	-0.04	6.5	-	-	-----	-----	-	-	-----	5.7	A	A
7.0	D	C-	.03	6.1	--	--	-----	-----	-	-	-----	-----	-	-	-----	-----	-	-
7.2	--	--	-----	-----	D+	C-	-0.03	8.5	C	C	-0.05	9.2	B	B	0.06	7.6	A	A
8.0	D	D	-----	-----	--	--	-----	-----	-	-	-----	-----	-	-	-----	-----	-	-
9.9	D	D	-----	-----	D+	D	-----	-----	C	C-	.01	14.0	B	B-	.03	13.7	A	A+

<sup>a</sup>Parachute behavior:

- A Parachute aligned itself with wind or at very small angles to the wind stream; very little motion.
- B Parachute aligned itself 50° to 100° to the wind stream and changed trim positions during flight.
- C Parachute assumed trim angles of 100° to 150° to the wind stream, changed trim position with an erratic motion.
- D Parachute assumed large angles of 150° to 200° to the wind stream and was in constant motion.

<sup>b</sup>Model stability:

- A Good.
- B Fair.
- C Poor.
- D Model unflyable.

<sup>c</sup> $\Delta C_L$  is the change in lift coefficient caused by the parachute being towed.

<sup>d</sup> $\Delta \gamma$  is the change in glide-path angle caused by the parachute being towed.



TABLE VII.

SPIN-RECOVERY-PARACHUTE TESTS MADE IN THE  
LANGLEY 20-FOOT FREE-SPINNING TUNNEL

Model	Steady spin parameters			Parachute			Towline length (in.)	D <sub>p</sub> (lb)	Turns required for recovery
	α <sub>s</sub> (deg)	V (fps)	Ω (rps)	Type	Diameter <sup>a</sup> (in.)	Porosity (cu ft/sq ft/min)			
2	63	44.9	1.0	Flat	9.00	Approx. 120	20	0.750	1, 1 $\frac{1}{4}$ , 1
				---do---	8.00	Approx. 120	20	.589	2 $\frac{1}{2}$ , 2, 2 $\frac{3}{4}$
				Hemi-spherical	5.86	150	20	.522	2, 1, 1 $\frac{1}{2}$ , 1 $\frac{3}{4}$ , 1 $\frac{1}{2}$
				---do---	5.86	250	20	.525	1 $\frac{1}{2}$ , 2, 1 $\frac{3}{4}$ , 1 $\frac{3}{4}$
3	56	44.9	1.9	---do---	5.86	400	20	.523	2 $\frac{1}{4}$ , 1 $\frac{1}{2}$ , 2 $\frac{1}{4}$ , 1, 2
				Flat	9.00	Approx. 120	20	.750	1, 1, 1
				Hemi-spherical	5.86	150	20	.522	1, 1 $\frac{1}{4}$ , 1, 1 $\frac{1}{4}$
				---do---	4.14	150	20	.272	2 $\frac{1}{4}$ , 2 $\frac{1}{4}$ , 2 $\frac{1}{4}$
4	32	49.8	2.0	Flat	9.00	Approx. 120	16	.922	4, 1, >5, 2 $\frac{1}{2}$
				Hemi-spherical	5.86	400	16	.644	1, 1 $\frac{1}{2}$ , 3 $\frac{1}{4}$ , 1
				Flat	10.60	Very high	16.6	.633	1 $\frac{3}{4}$ , 1 $\frac{1}{2}$ , 1 $\frac{1}{4}$ , 1 $\frac{1}{4}$ , 2
				Flat	6.00	Approx. 120	15	.492	1 $\frac{3}{4}$ , 1 $\frac{1}{2}$ , 1 $\frac{1}{2}$ , 2, 1
5	b <sub>30</sub> to 50	Approx. 54.0	(b)	Hemi-spherical	4.14	150	15	.393	1 $\frac{1}{2}$ , 1 $\frac{1}{2}$ , 1, 1 $\frac{1}{2}$
				---do---	4.20	250	15	.404	1 $\frac{1}{2}$ , 1 $\frac{1}{2}$ , 1 $\frac{1}{2}$
				---do---	4.20	400	15	.391	1, 1 $\frac{1}{2}$ , 3 $\frac{1}{4}$ , 1 $\frac{1}{4}$ , 2

<sup>a</sup>Preformed diameter for hemispherical parachutes; laid-out-flat diameter for flat parachutes.

<sup>b</sup>Oscillatory spin; difficult to control model in tunnel.

<sup>c</sup>Porosity was not measured but probably exceeded 900. This parachute had a strip of imporous tape 1 inch wide attached around its edge above the rim.



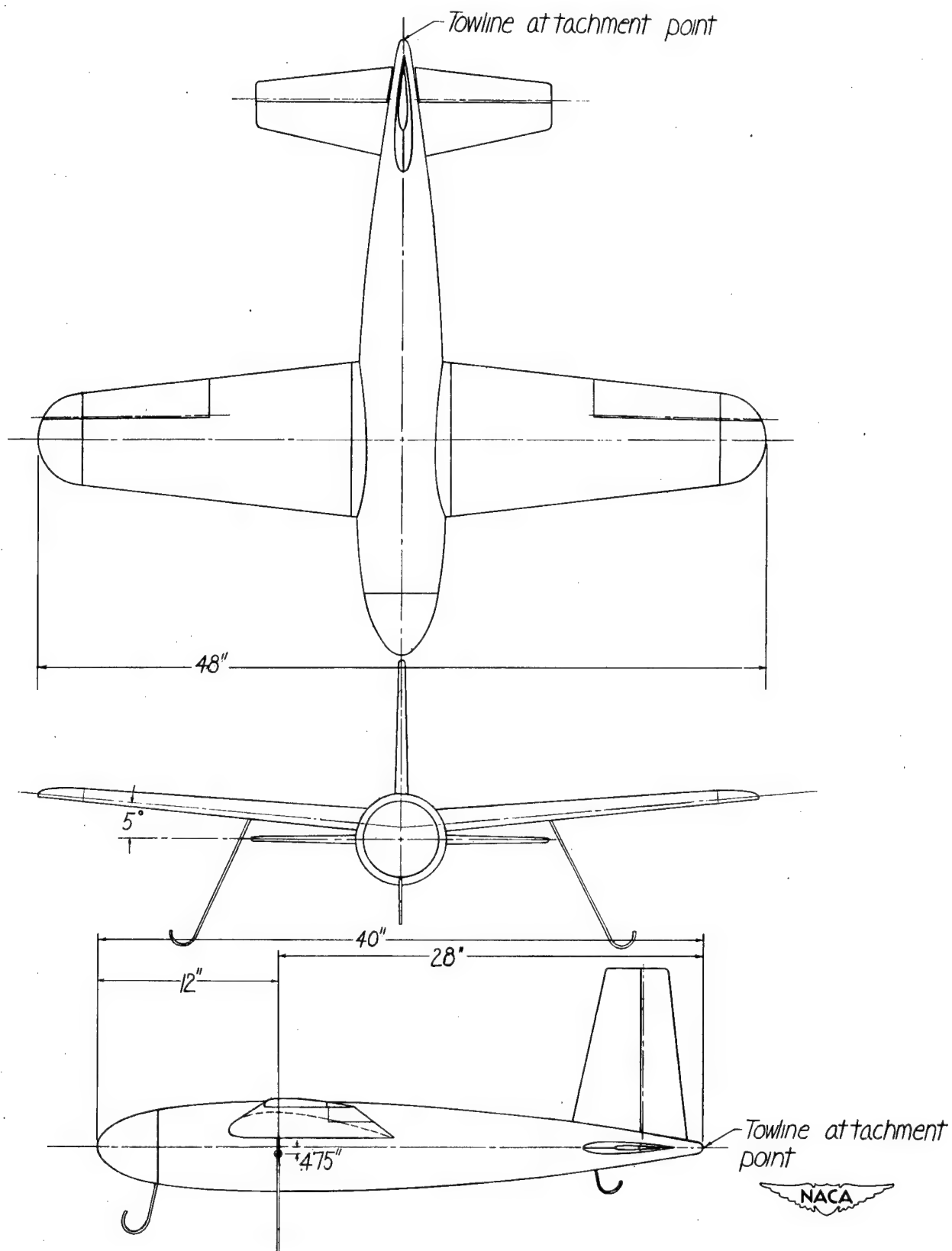


Figure 1.- Three-view drawing of model 1 used for towing parachutes in Langley free-flight tunnel.

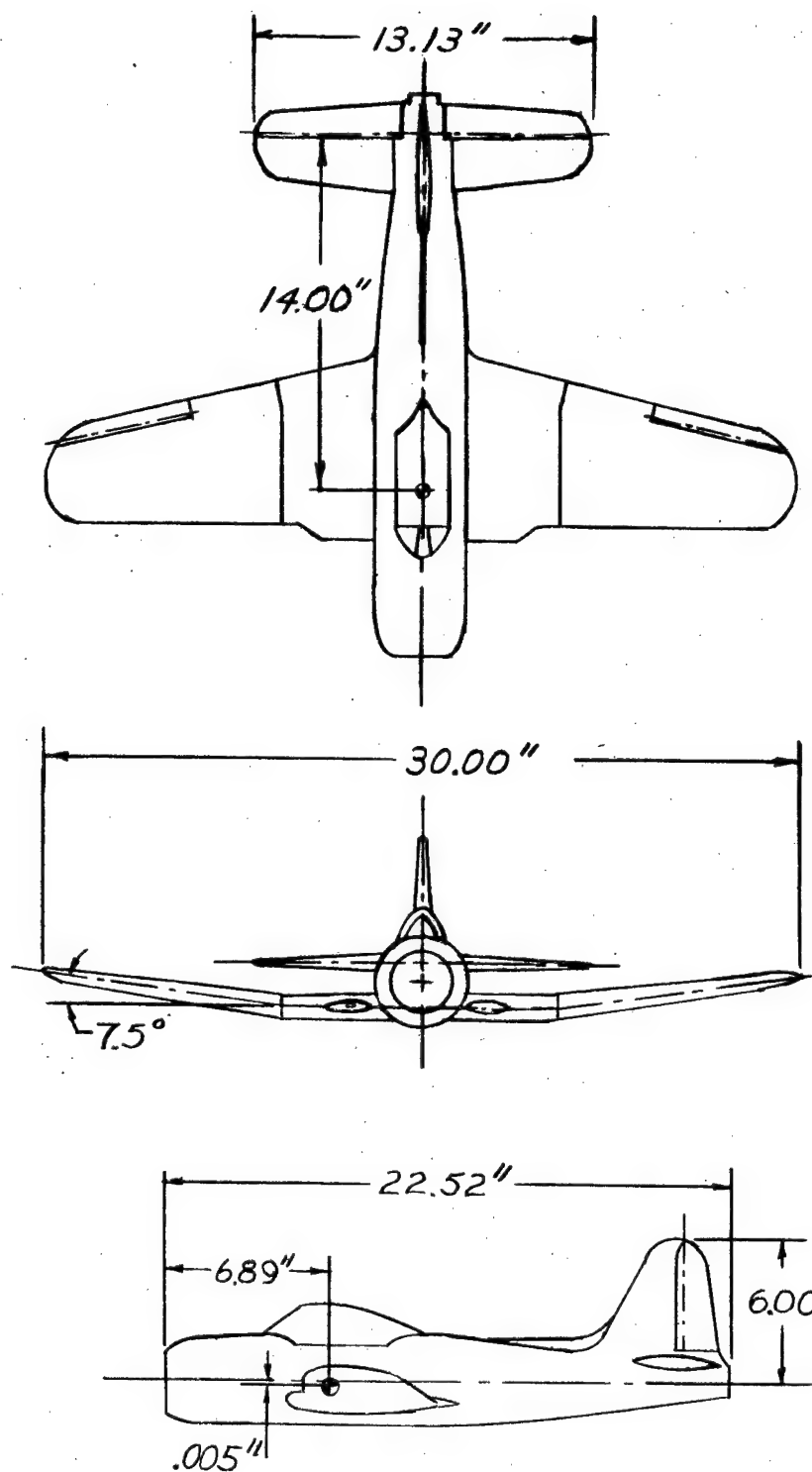


Figure 2.- Three-view drawing of model 2, used for spin-recovery-parachute tests in Langley 20-foot free-spinning tunnel.

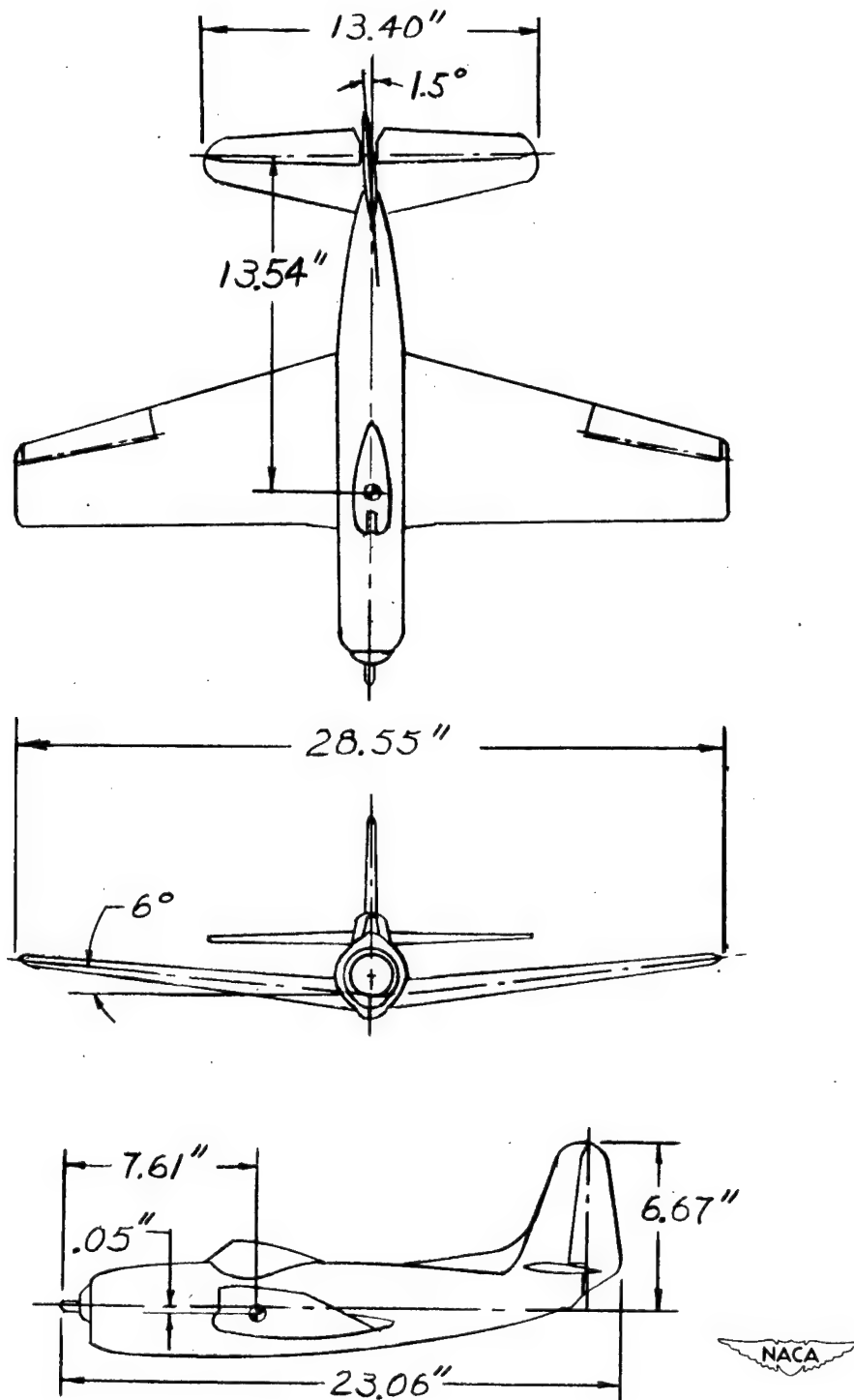


Figure 3.- Three-view drawing of model 3, used for spin-recovery-parachute tests in Langley 20-foot free-spinning tunnel.

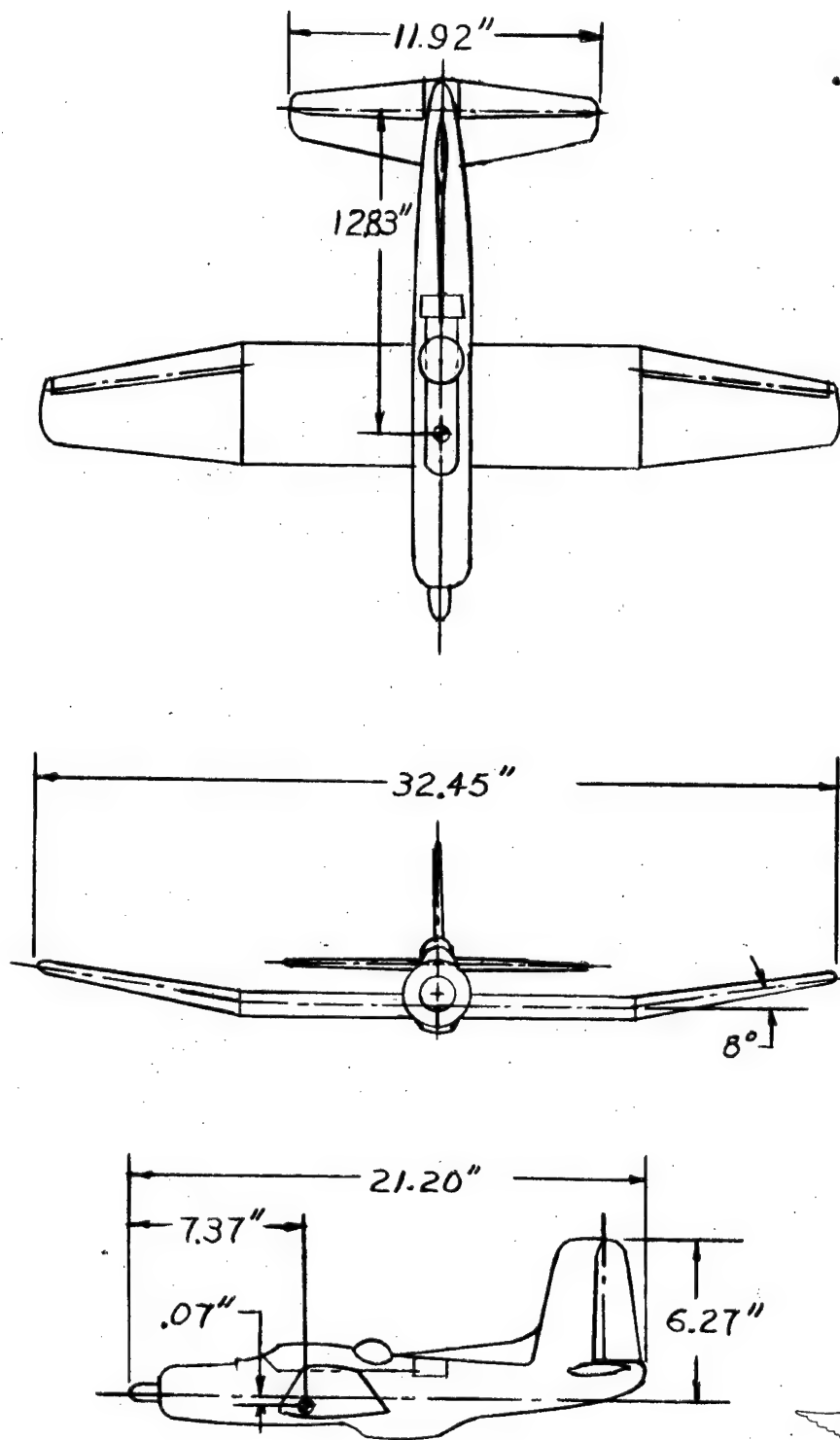


Figure 4.- Three-view drawing of model 4, used for spin-recovery-parachute tests in Langley 20-foot free-spinning tunnel.

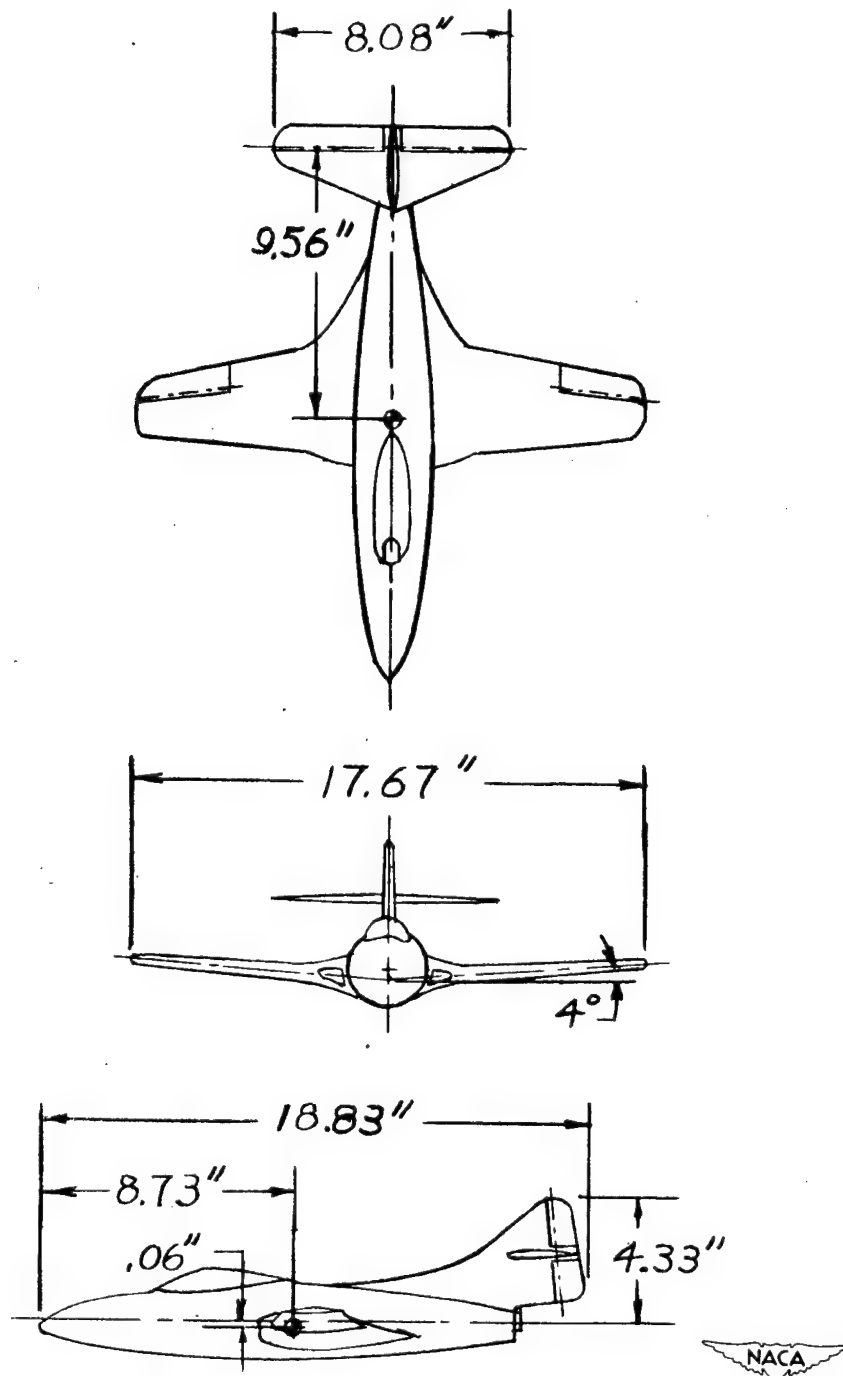


Figure 5.- Three-view drawing of model 5, used for spin-recovery-parachute tests in Langley 20-foot free-spinning tunnel.

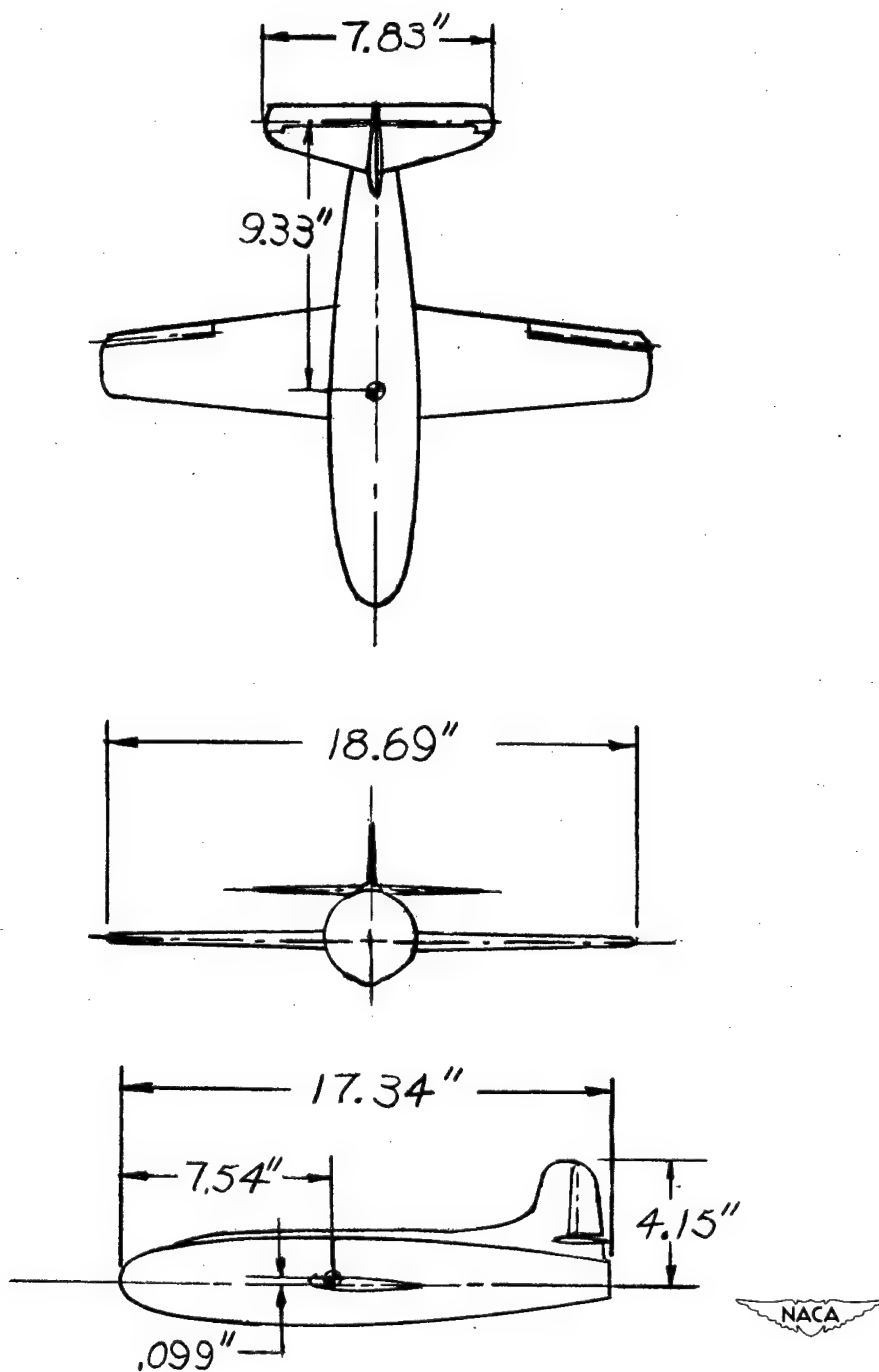


Figure 6.- Three-view drawing of model 6, used in Langley 20-foot free-spinning-tunnel tests to determine effect of lengthening towline of a conventional flat parachute.

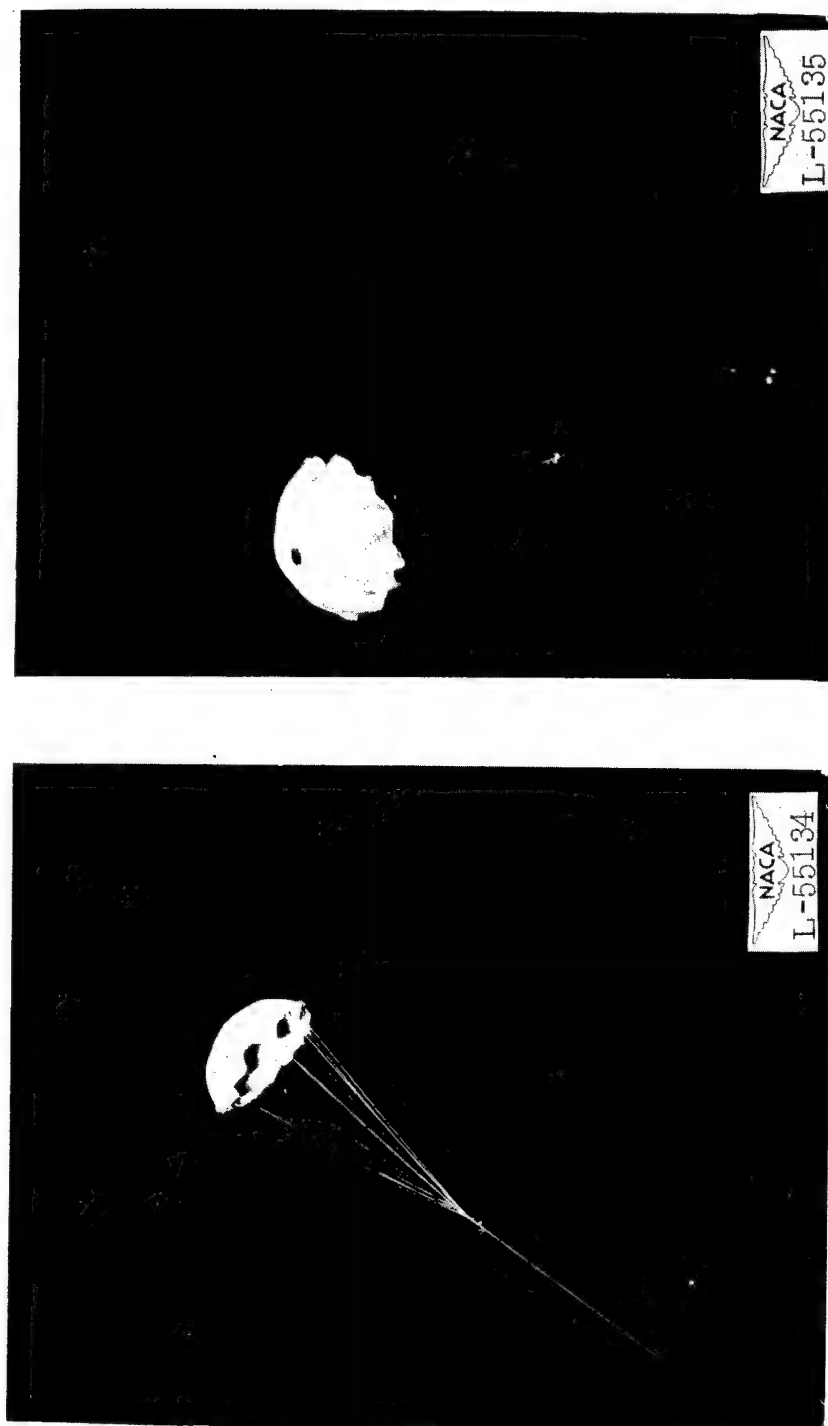


Figure 7.- An unstable flat parachute open in vertically rising air stream  
of Langley 20-foot free-spinning tunnel.

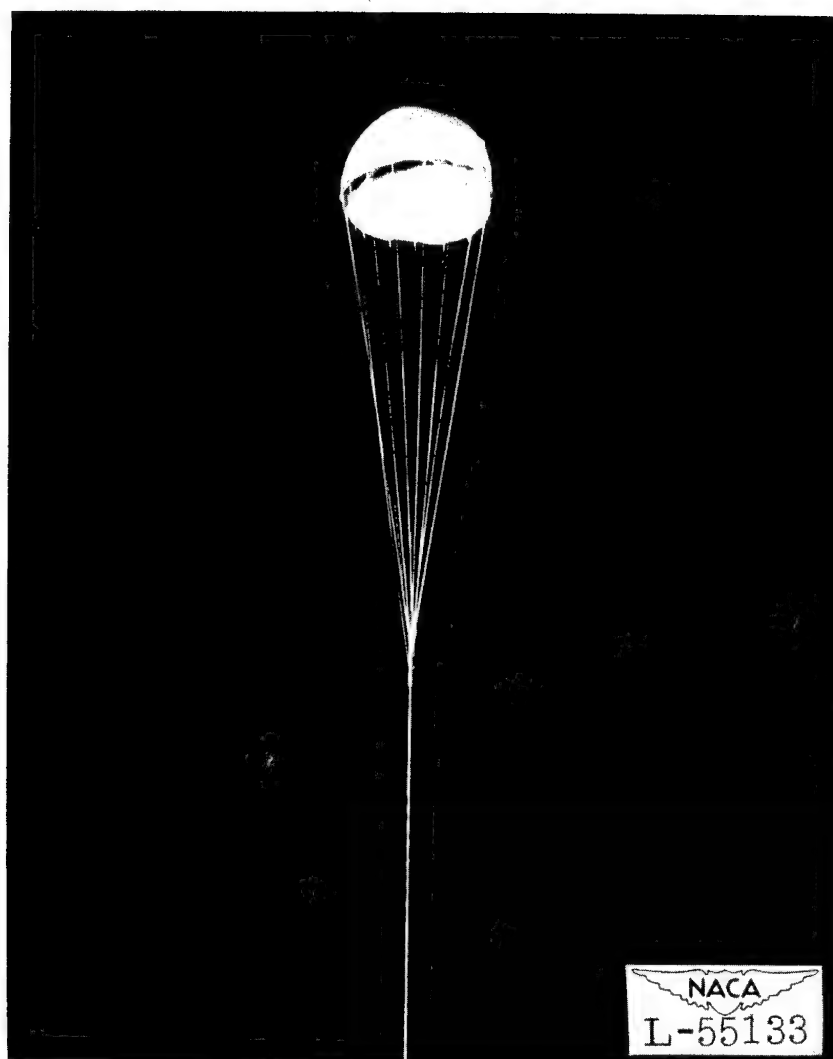


Figure 8.- A stable hemispherical parachute open in vertically rising air stream of Langley 20-foot free-spinning tunnel.

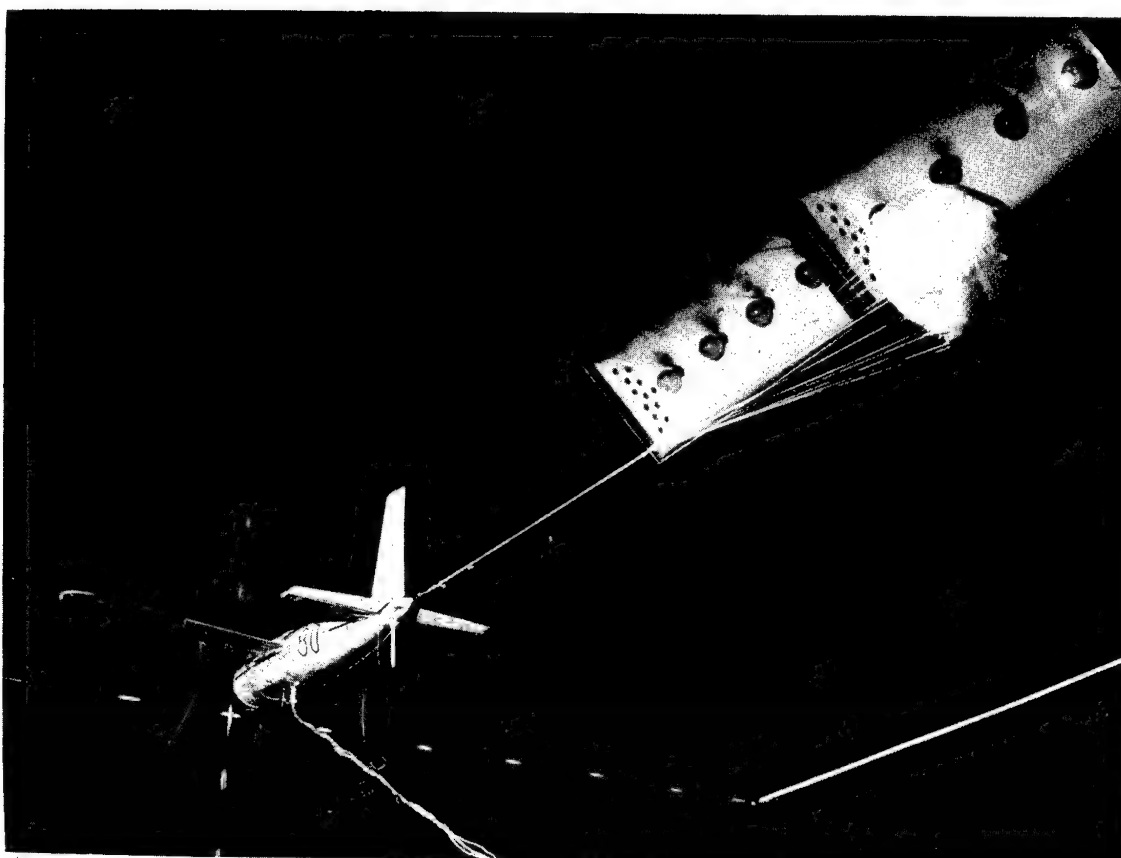


Figure 9.- Model 1 towing a 7.23-inch-diameter stable hemispherical parachute in Langley free-flight tunnel.

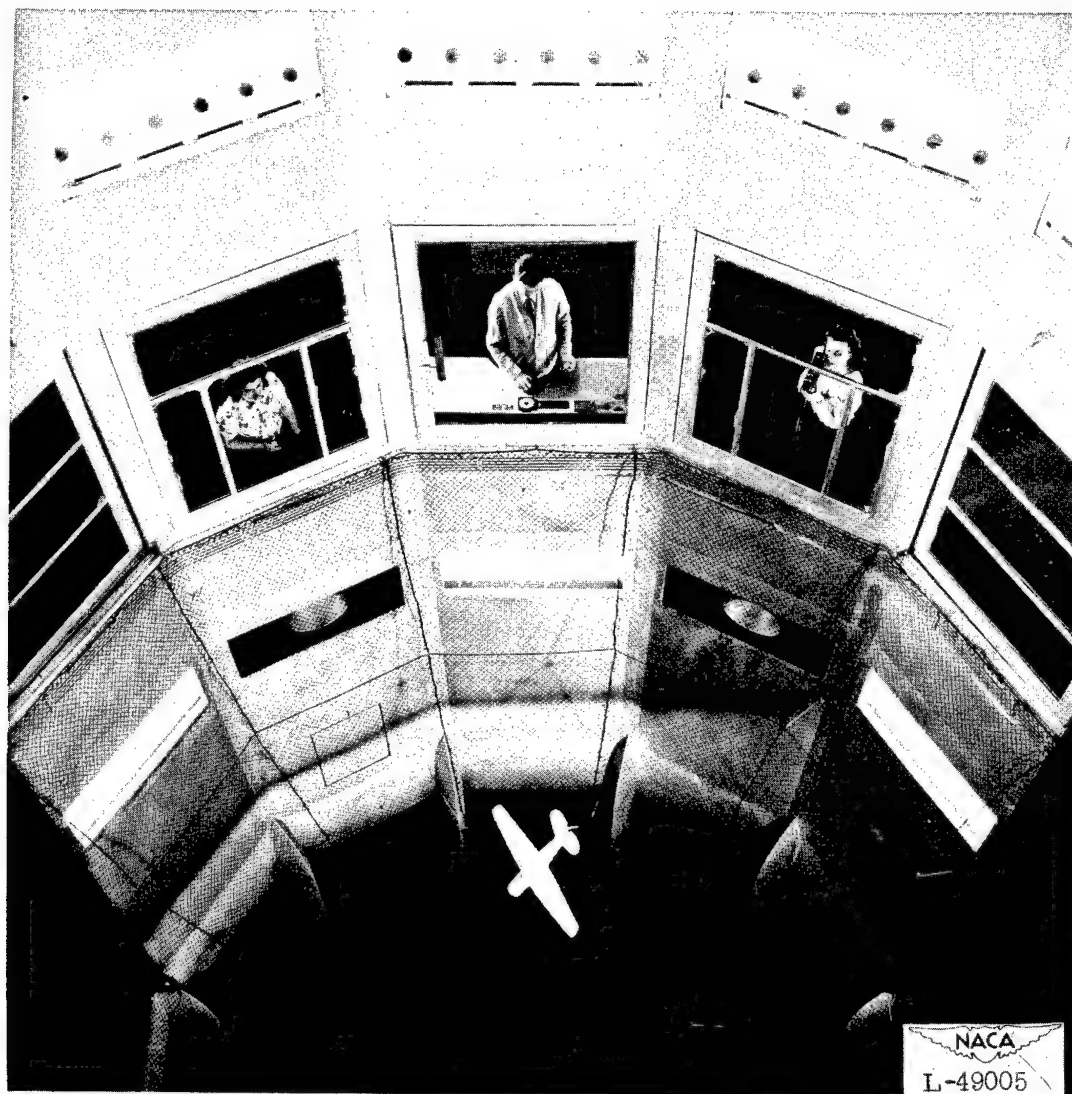


Figure 10.- A typical airplane model spinning in Langley 20-foot free-spinning tunnel.

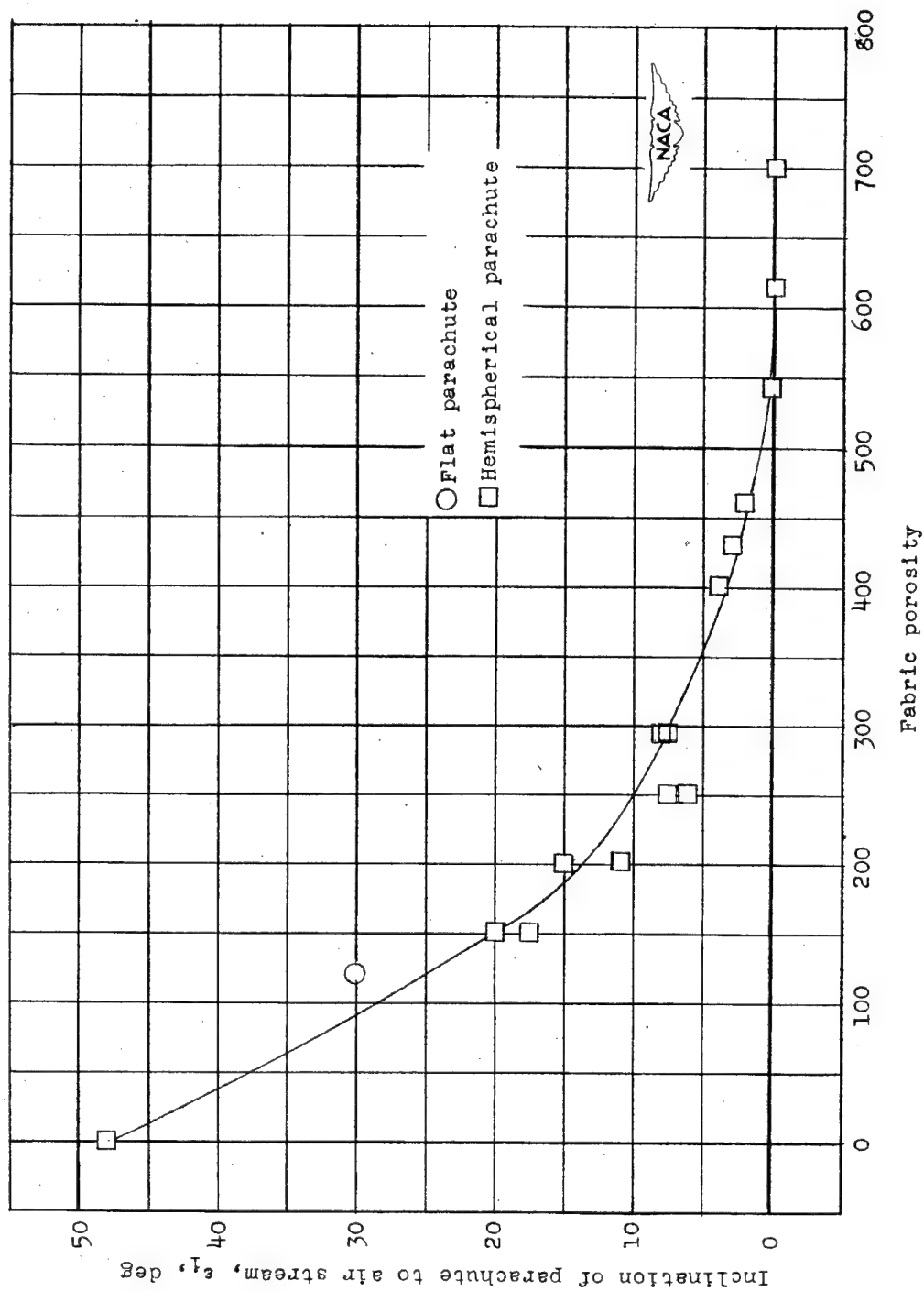


Figure 11.- Variation of angle of inclination to air stream with porosity for hemispherical and flat parachutes tested in Langley 20-foot free-spinning tunnel.

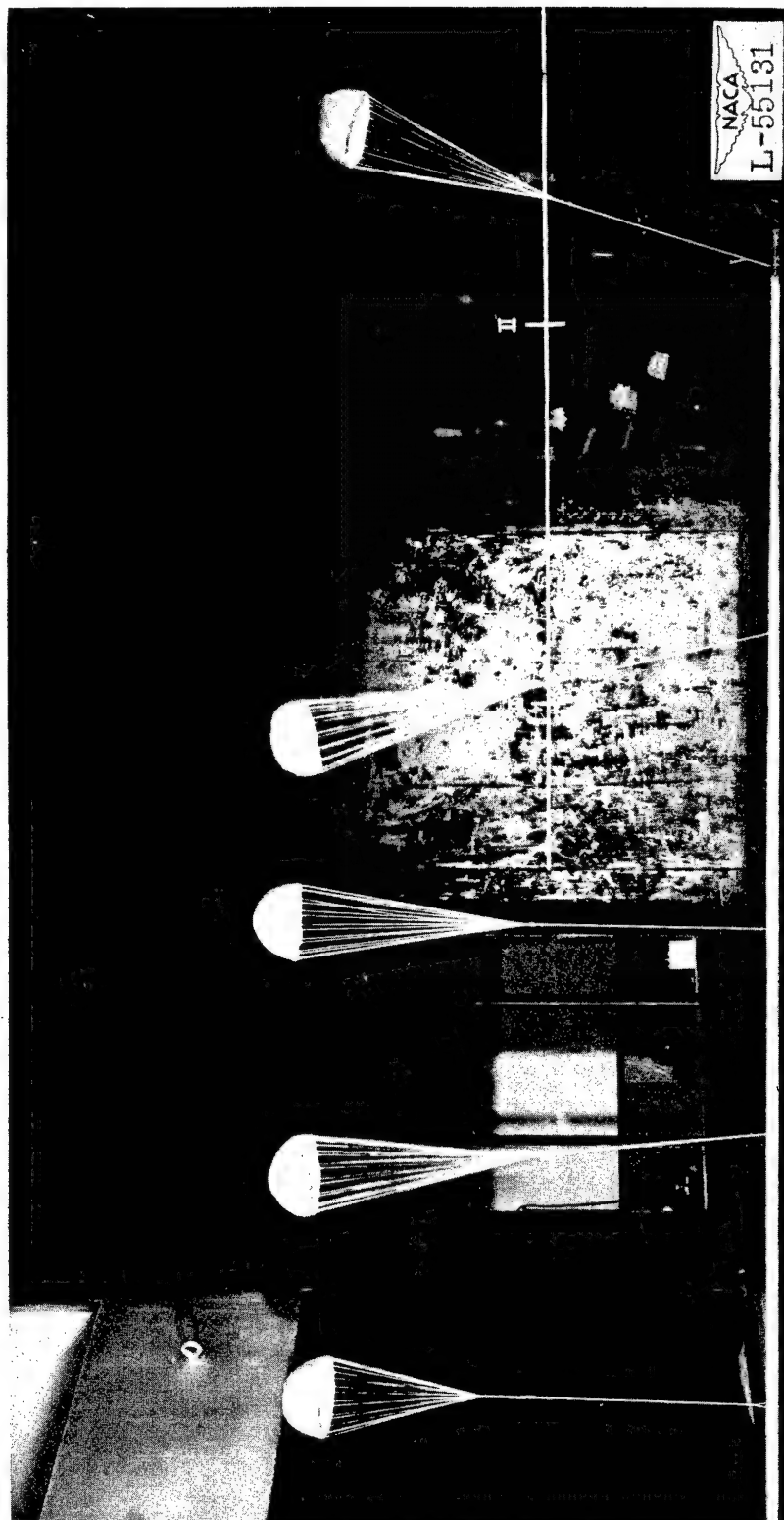


Figure 12.- Five approximately 9.80-inch-diameter hemispherical parachutes with porosity numbers (left to right) of 400, 294, 250, 200, and 150 being tested in Langley 20-foot free-spinning tunnel. Parachute with porosity of 250 is inclined toward camera.

Frames 1 to 11

12 to 22

23 to 33

34 to 44

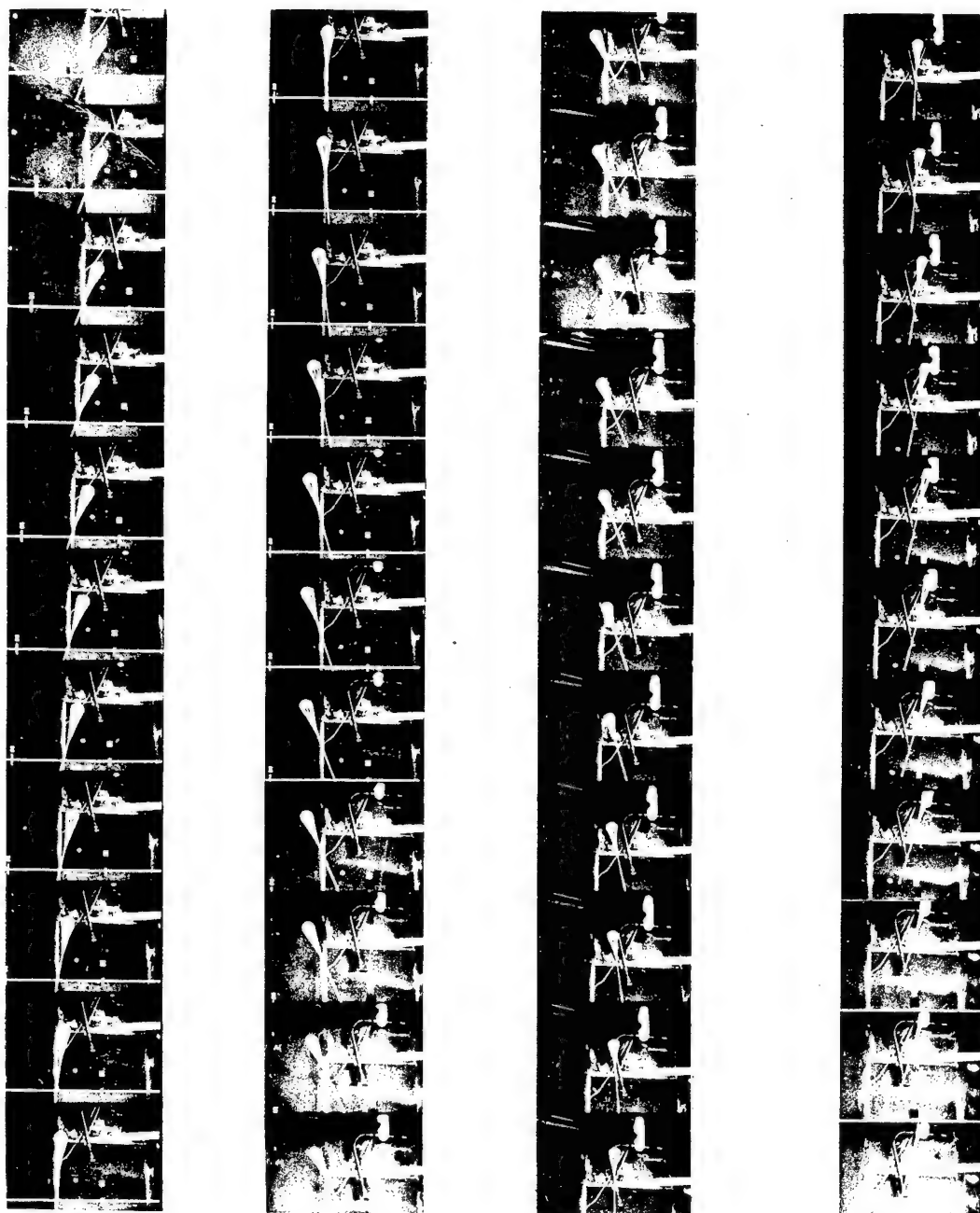


Figure 13.- Motion-picture strip of the 5.86-inch-diameter 150-porosity hemispherical parachute - with a weight attached to its towline - floating freely in vertically rising air stream of Langley 20-foot free-spinning tunnel. The pictures were made at a camera speed of 32 frames per second.

45 to 55



56 to 66



67 to 77



78 to 88

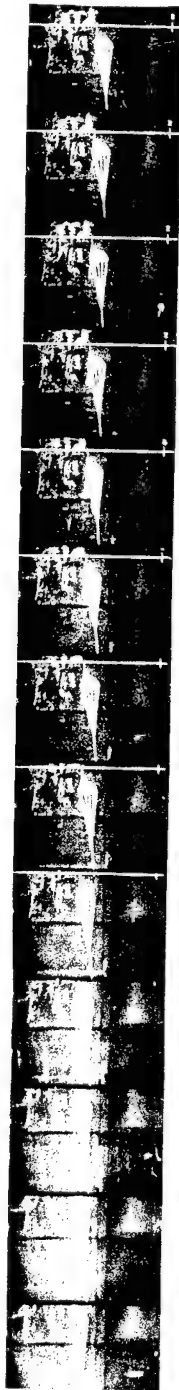


Figure 13.- Concluded.

Frames 1 to 13



14 to 26



27 to 39



40 to 52



Figure 14.- Motion-picture strip of the 5.86-inch-diameter 400-porosity hemispherical parachute - with a weight attached to its towline - floating freely in vertically rising air stream of Langley 20-foot free-spinning tunnel. The pictures were made at a camera speed of 32 frames per second.

53 to 65



66 to 78



79 to 91



92 to 104



Figure 14.- Concluded.

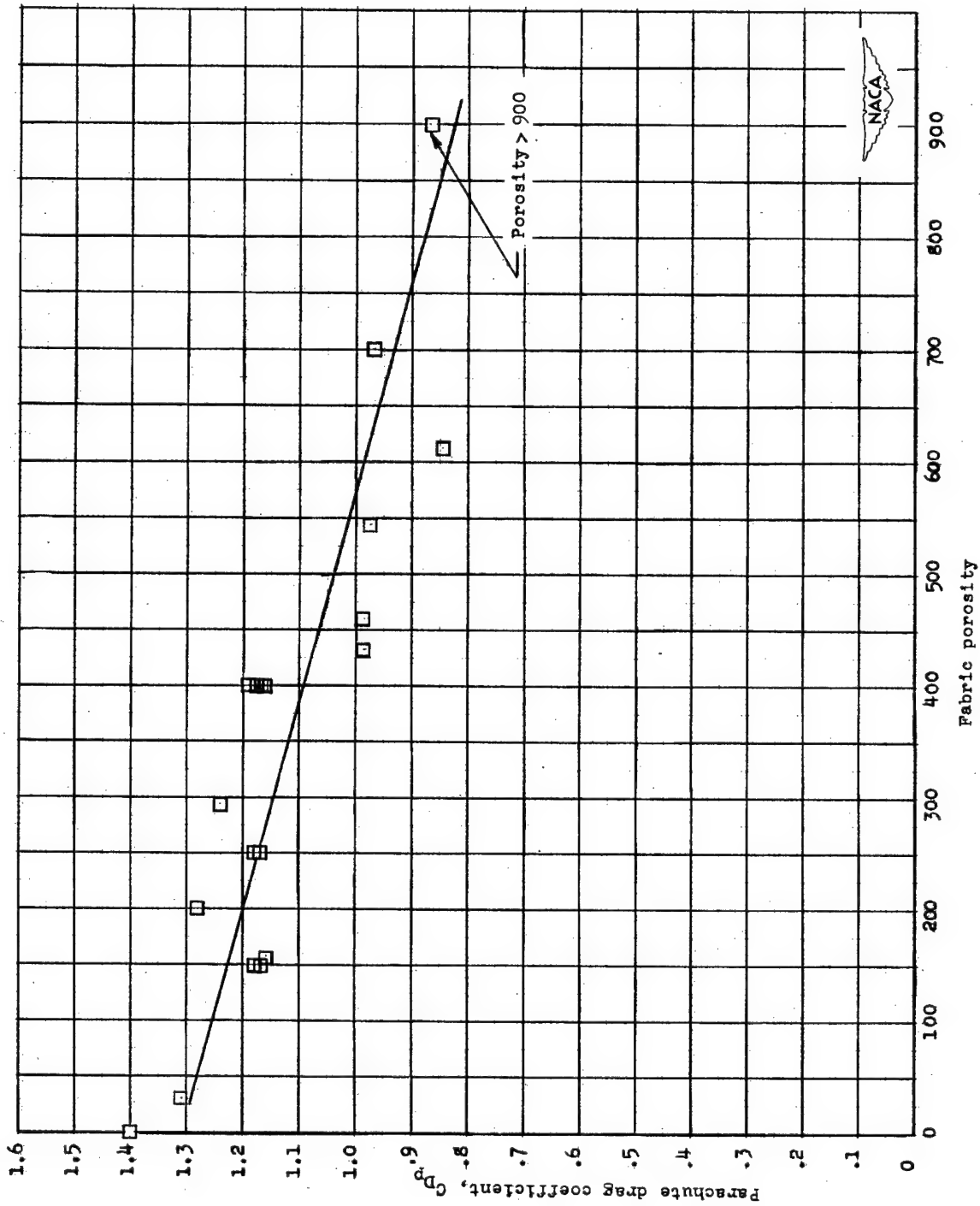


Figure 15.- Variation of parachute drag coefficient with porosity for hemispherical parachutes tested in Langley 20-foot free-spinning tunnel.

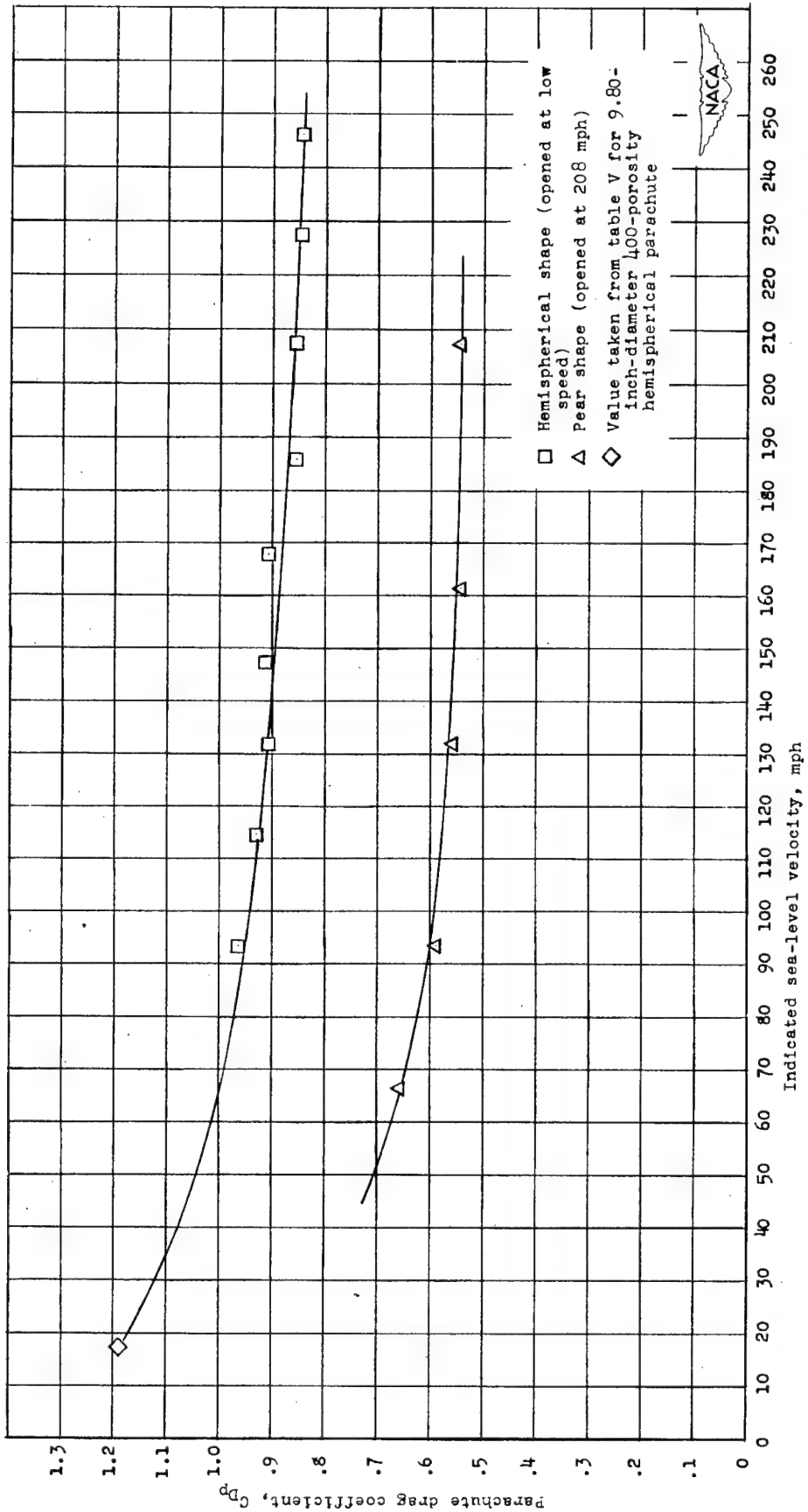


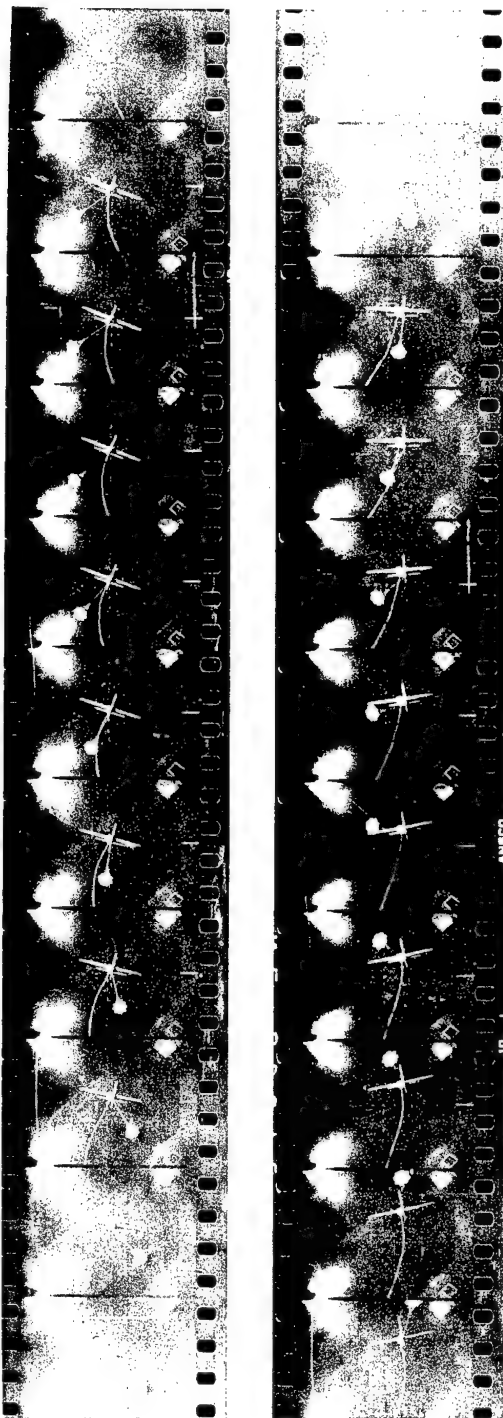
Figure 16.- Variation of parachute drag coefficient with indicated sea-level velocity for 11.84-inch-diameter 400-porosity hemispherical parachute tested in Langley 300 MPH 7- by 10-foot tunnel.

Frames 1 to 11

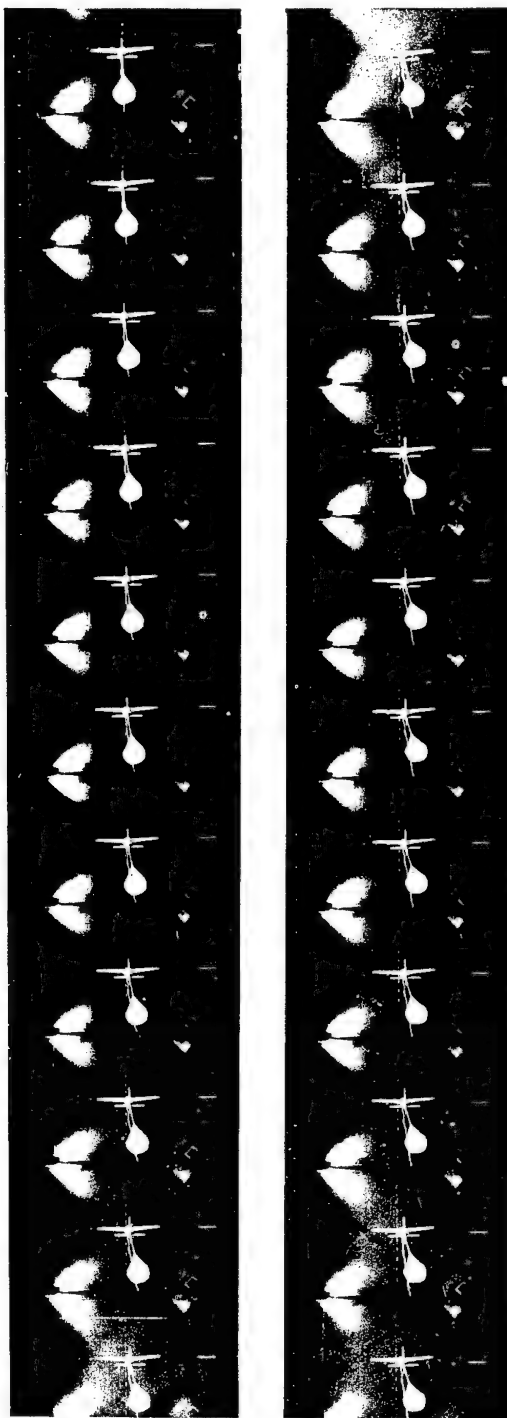
12 to 22

Frames 1 to 11

12 to 22



Unstable



Stable

Figure 17.- Motion-picture strip of unstable 5.70-inch-diameter flat parachute and stable 7.23-inch-diameter hemispherical parachute being towed in gliding flight in Langley free-flight tunnel. The pictures were made at a camera speed of 32 frames per second.

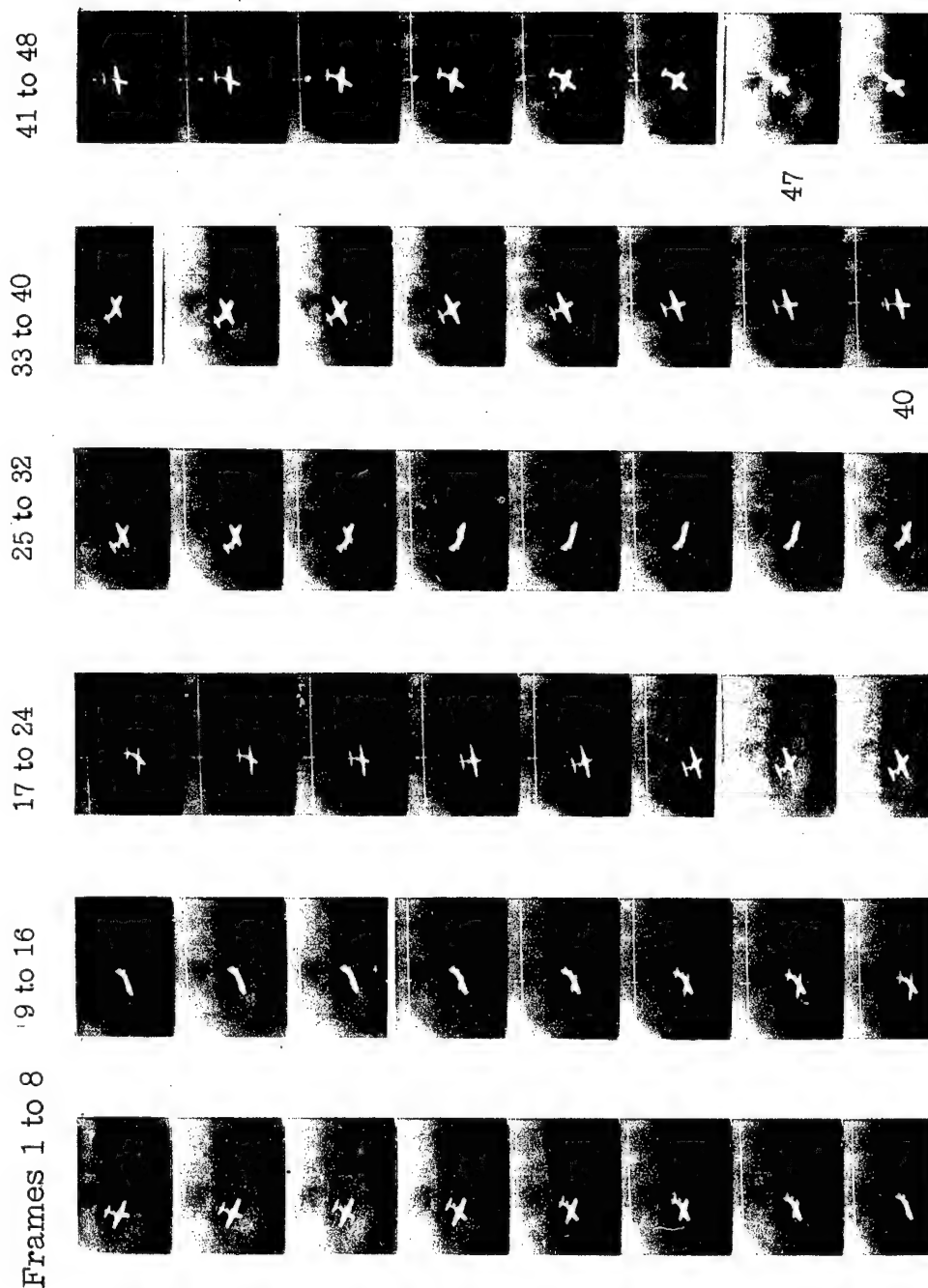
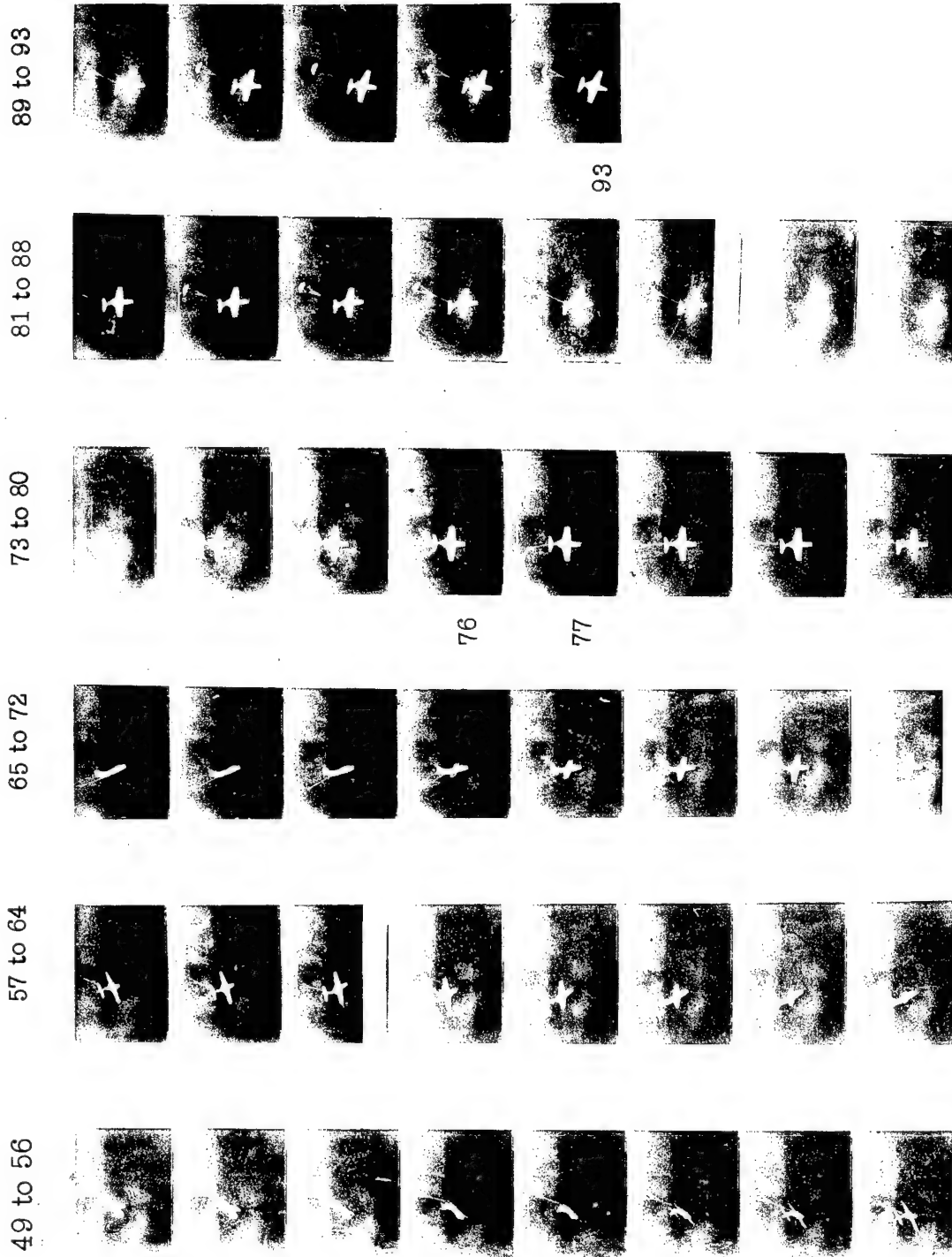


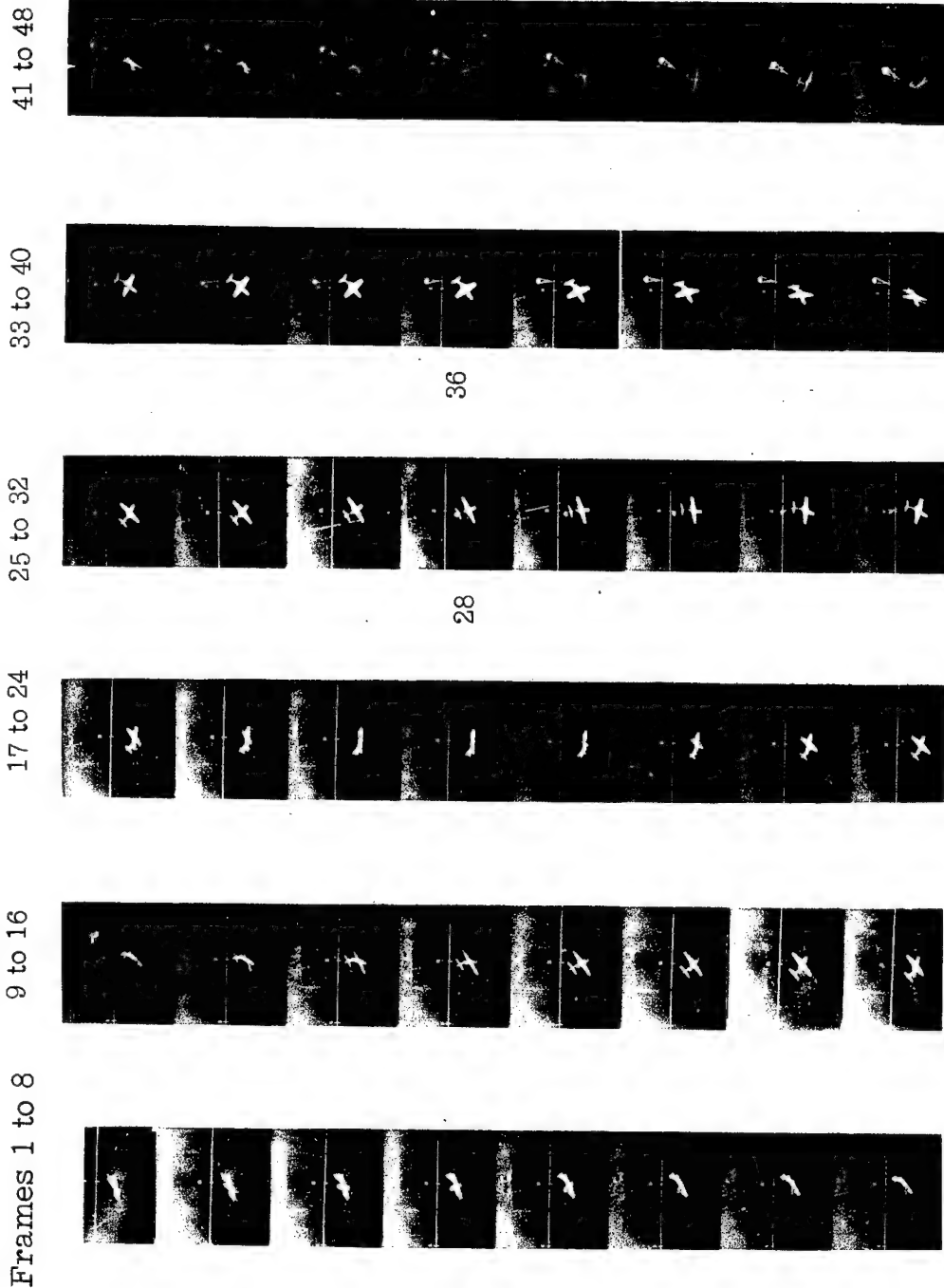
Figure 18.- Motion-picture strip of model 5 recovering from a spin after 6.00-inch-diameter conventional flat parachute was opened. Parachute pack started to open at frame 40. Parachute had opened fully at frame 47. Model had recovered from spin at frame 76. Model in recovery dive during frames 77 to 93. The pictures were made at a camera speed of 32 frames per second.

NACA  
L-56338



NACA  
L-56339

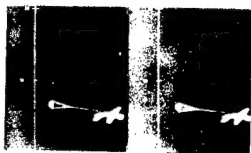
Figure 18.- Concluded.



NACA  
L-56340

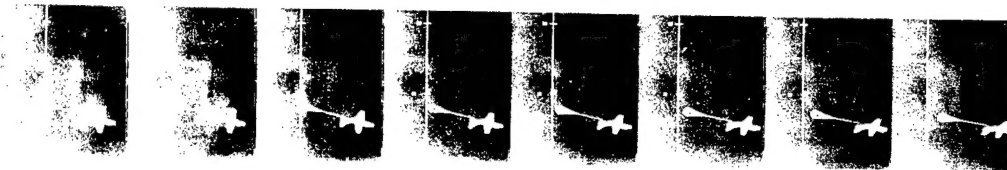
Figure 19.- Motion-picture strip of model 5 recovering from a spin after 4.20-inch-diameter 400-porosity hemispherical parachute was opened. Parachute pack started to open at frame 28. Parachute had opened fully at frame 36. Model had recovered from spin at frame 70. Model in recovery dive during frames 71 to 82. The pictures were made at a camera speed of 32 frames per second.

81 to 82



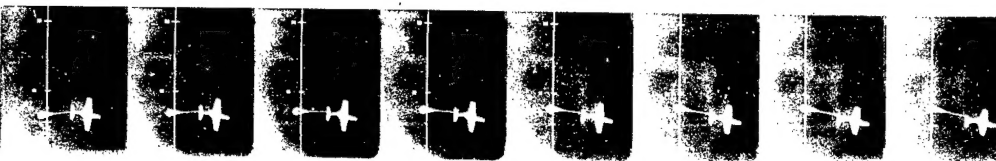
82

73 to 80



NACA  
L-56341

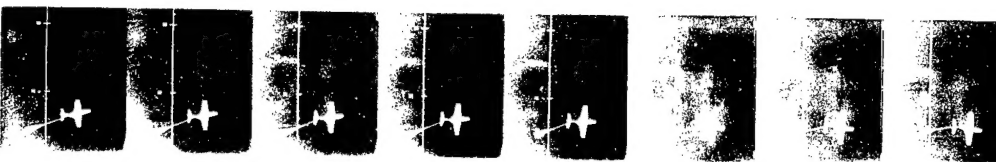
65 to 72



70

71

57 to 64



49 to 56



Figure 19.- Concluded.

Frames 1 to 12



13 to 24



25 to 36



37 to 48

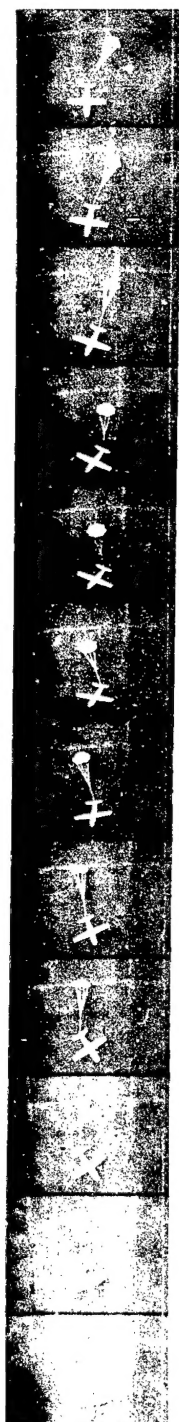


Figure 20.- Motion-picture strip of model 6 suspended with a 10-inch towline from 10.00-inch-diameter flat parachute (porosity approximately 120) in vertically rising air stream of Langley 20-foot free-spinning tunnel. The pictures were made at a camera speed of 32 frames per second.

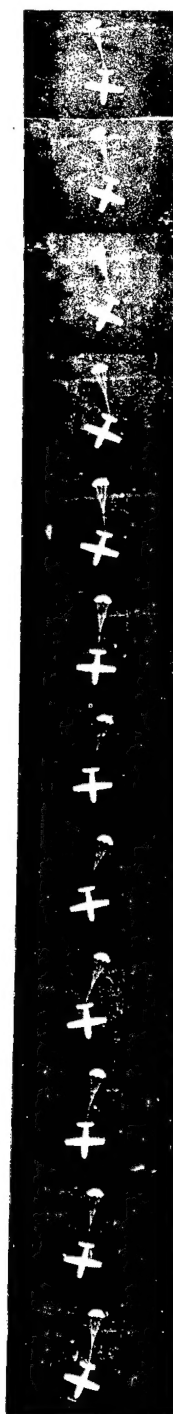
49 to 60



61 to 72



73 to 84



85 to 96

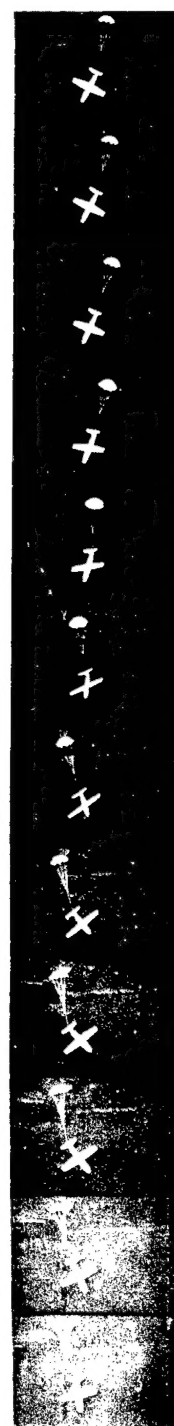


Figure 20.- Concluded.

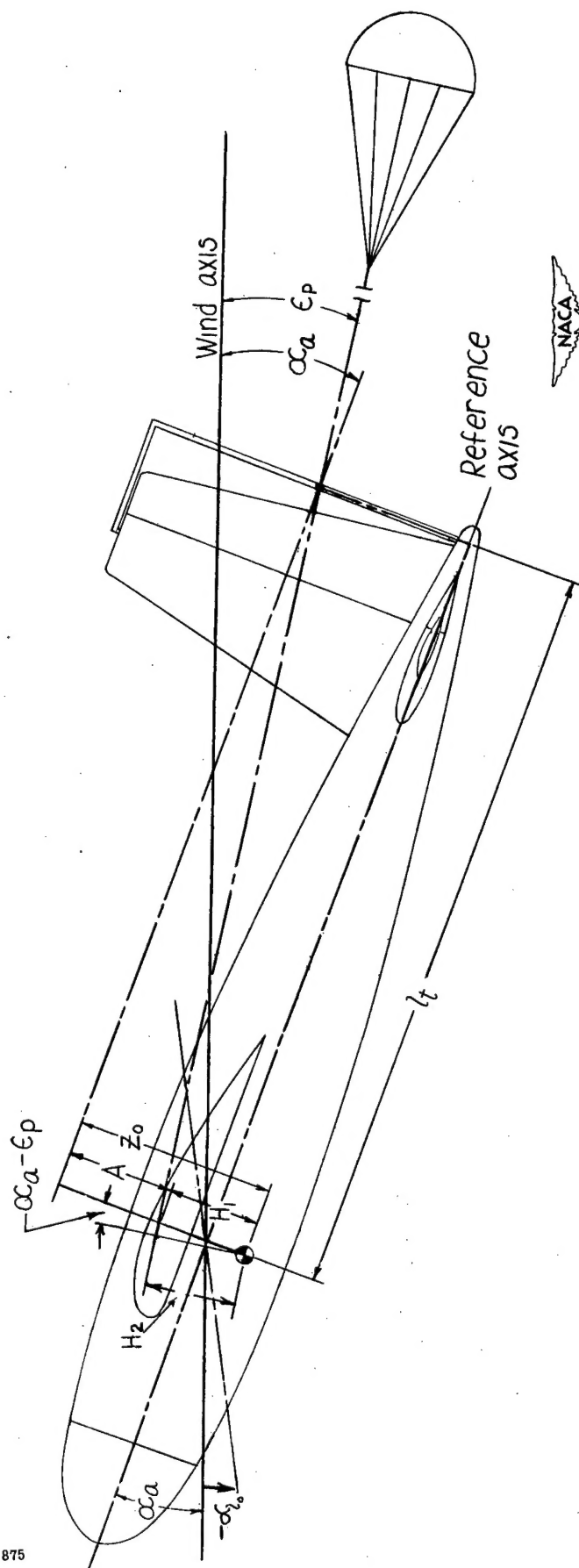


Figure 21.- Sketch of model with tail parachute showing angles and distances used in calculating increases in stability of model resulting from parachute.